Digitally Programmable Tuned Circuits

by

Muhammad Haroon Khan

A Thesis Presented to the

FACULTY OF THE COLLEGE OF GRADUATE STUDIES

KING FAHD UNIVERSITY OF PETROLEUM & MINERALS

DHAHRAN, SAUDI ARABIA

In Partial Fulfillment of the
Requirements for the Degree of

MASTER OF SCIENCE

In

ELECTRICAL ENGINEERING

October, 1994

Digitally Programmable Tuned Circuits

BY

Muhammad Haroon Khan

A Thesis Presented to the

FACULTY OF THE COLLEGE OF GRADUATE STUDIES

KING FAHD UNIVERSITY OF PETROLEUM & MINERALS

DHAHRAN, SAUDI ARABIA

In Partial Fulfillment of the
Requirements for the Degree of

MASTER OF SCIENCE

In

Electrical Engineering

October 1994

KING FAHD UNIVERSITY OF PETROLEUM AND MINERALS
DHAHRAN, SAUDI ARABIA

This thesis, written by

Muhammad Haroon Khan

under the direction of his Thesis Advisor, and approved by his Thesis committee, has been presented to and accepted by the Dean, College of Graduate Studies, in partial fulfillment of the requirements for the degree of

MASTER OF SCIENCE IN ELECTRICAL ENGINEERING

Thesis Committee:

30/11/94

Dr. M. T. Abuelma'atti (Chairman)

Dr. A. R. K. Al-Ali (Co-Chairman)

5/12/94

Dr. I. M. Naqvi (Member)

30/11/1994

Dr. Z. J. Saati (Member)

Dr. J. Zrida (Member)

Department Chairman

Dr. Ala H. Rabeh
Dean, College of Graduate Studies

Date: 7/12/94

Dedicated to

the memory of my mother

Acknowledgment

In the name of Allah, Most Gracious, Most Merciful. Read in the name of thy Lord and Cherisher, Who created. Created man from a {*leech-like* } clot. Read and thy Lord is Most Bountiful. He Who taught {the use of} the pen. Taught man that which he knew not. Nay, but man doth transgress all bounds. In that he looketh upon himself as self-sufficient. Verily, to thy Lord is the return {of all}.

(The Holy Quran, Surah 96)

First and foremost, all praise to the Almighty Allah Who gave me the courage and patience to carry out this work successfully.

Acknowledgement is due to King Fahd University of Petroleum and Minerals for providing support to this work.

My deep appreciation goes to my major thesis advisor Dr. M. T. Abuelma'atti for his constant help, guidance and the countless hours of attention he devoted throughout the course of this work. He was always kind, understanding and sympathetic towards me. Working with him was indeed a wonderful and learning experience which I thoroughly enjoyed.

Thanks are due to my thesis co-advisor Dr. Al-Ali and committee members Dr. Naqvi, Dr. Saati and Dr. Zrida for their interest and co-operation. In particular, I owe a cosiderable debt to Dr. Al-Ali for his invalulable support, help and encouragement which he rendered to me.

I am also grateful to the department chairman, Dr. Abdallah Al-Shehri and other faculty members for their support.

Acknowledgement and thanks are due to my family members for their understanding throughout my academic career.

I would also like to acknowledge the assistance and support that I received from Shahid Tanvir, Asaf Maruf and Khalid Abdulaziz during the compilation of this thesis. Another word of thanks must go to all my friends on the campus especially (in alphabatical order), Abbas, Adnan, Cheema, Fahim, Iftikhar, Irfan, Neaz Sahab, Rana, Rizwan, Sami, Sayani and Waheed who made my stay at KFUPM a pleasant experience.

I also remain grateful to Lab-technicians Mr. Farazi, Mr. Shams, Mr. Joey and Secretary COE department, Mr. Khursheed, for their support and cooperation.

Last but not least, I wish to thank the computer engineering department, especially Dr. Benten, for letting me use their wonderful computing facilities.

Contents

List of Tables

List of Figures

Abstract

Name: Muhammad Haroon Khan

Title: Digitally Programmable Tuned Circuits

Major Field: Electrical Engineering

Date of Degree: October, 1994

In this thesis, a number of simulator circuits synthesizing capacitors and inductors have been discussed. The programmable feature of the operational transconductance amplifiers (OTAs) has been exploited to advantage to make the simulator circuits voltage/current controlled and consequently controllable by the output of a digital to analog converter (DAC). This results in digitally programmable tuned circuits. The temperature sensitivity of the OTAs has been countered to make the overall circuit temperature-independent (independent of the V_T term), resulting in Digitally Programmable Temperature-Independent Tuned (DiPTIT) circuits. The stability of some of these circuits has been discussed to show how non-idealities of active elements play an important role in determining the performance of such circuits.

Master of Science Degree

King Fahd University of Petroleum and Minerals

Dhahran, Saudi Arabia

October 1994

خلاصة الرسالة

الاسم	:	محمد هارون خان
عنوان الرسالة	:	دوائر الكترونية مبرمجه رقميا
التخصص	:	الهندسة الكهربائية
تاريخ الشهادة	:	اكتوبر ١٩٩٤م

فى هذه الاطروحه تم مناقشه وعرض عدد من الدوائر الالكترونية للحصول على مكثفات و ملفات باستخدام خاصيه البرمجه المتوفره فى دوائر مكبرات عمليات التحويل من جهد الى تيار. وهذا يساعد على برمجه الملفات و المكثفات رقميا عن طريق جهد رقمى يتم تحويله الى جهد تمثيلى من خلال محول رقمى/تمثيلى. وقد تم التغلب على احد العيوب الرئيسية فى المكبرات المذكوره و هو تغير خصائصها مع تغير درجه الحراره و اصبح من الممكن الحصول على ملفات و مكثفات مبرمجة رقميا و لا تتأثر بتغير درجه الحراره. و نظرا لأهميه توفر الاستقرار لهذه الدوائرفقد تمت دراسه تأثير الخصائص غير المثاليه للمكبرات على عمل بعض الدوائر المتقدمة.

درجة الماجستير فى العلوم
جامعة الملك فهد للبترول و المعادن
الظهران - المملكة العربية السعودية
اكتوبر ١٩٩٤م

Chapter 1

Introduction

1.1 Overview

Tuned circuits play an important role in electronics. In a number of applications, such as in the design of radio and TV receivers, the need arises for an amplifier whose frequency response peaks around a certain frequency (called the center frequency) and falls off on both sides of this frequency. Amplifiers with such a response are called tuned amplifiers, bandpass amplifiers, or bandpass filters.

A tuned amplifier forms the heart of the front-end or tuner of a communication receiver. By adjusting its center frequency to coincide with the frequency of a desired communication channel, the signal of this particular channel can be received while those of other channels are attenuated or filtered out. The basic principle underlying the design of tuned amplifiers is the use of a parallel RLC circuit as the load, or at

the input, of a BJT or a FET amplifier.

Fig. 1.1 shows the frequency response of a tuned amplifier, which, in fact, is similar to the frequency response of a bandpass filter. The response shows a center frequency ω_o with 3-dB bandwidth B. The frequency ω_o depends upon the value of L and C and is called the resonance frequency of parallel RLC resonator circuit. In fact, the parallel LC circuit form a frequency-selective network which controls the value of ω_o.

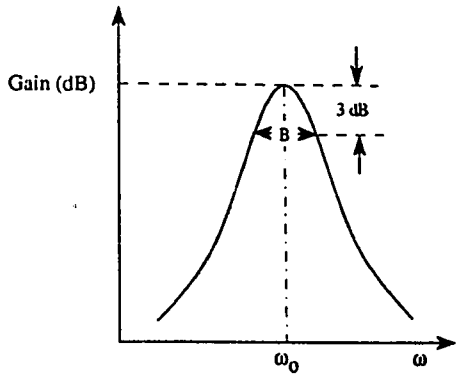

Figure 1.1: Frequency response of a tuned amplifier.

In addition to the use of tuned circuits in radio-frequency (RF) and intermediate-frequency (IF) section of communication systems they also find application in designing different types of filters and variable frequency oscillators. Tuned circuits are used in the design of oscillators to produce signals of various frequencies. These oscillator circuits employ a positive-feedback loop consisting of an amplifier and an RC or an LC tuned frequency-selective network.

A tuned circuit is said to be passive if it uses passive R, L and C components only. On the other hand if they are realized by an active device (op-amp), only RC circuits can be used. This is because the performance of an inductor is in fact simulated by the op amp and the RC circuit. In the first case, in fact, the LC network form the frequency-selective network and is thus responsible for the upper and lower corner frequencies of the filter. In other words, the corner frequencies are determined by the values of L and C in the circuit, and by changing their values, we can control the characteristics of the filter. In the second case, the RC-active network performs the same job.

Techniques such as immitance simulator networks and general impedance converters (GICs) have been developed to simulate positive and negative inductors, resistors and resistively controlled capacitors using active devices. These simulated components have been used in place of passive components in various tuned circuits to obtain electronic tunability and achieve reduction in the size of the circuit (e.g. physical inductors are large sized and bulky). The value of the simulated component depends on some other parameters of the circuit such as resistance, capacitance or the transconductance (g_m) of an operational transconductance amplifier (OTA). Since the g_m of an OTA can be controlled by a voltage (or current), hence the value of the simulated component can be varied by this control voltage or current thereby making the circuit electronically tunable.

1.2 Literature Review

1.2.1 Inductor Simulator Circuits

Kumar et al. have reported in [1] that inductors using ferromagnetic materials are bulky and costly, but a reduction in the size of the inductor reduces the quality factor. There also exist fundamental limitations on the realization of inductances for microminiature and integrated circuit applications. As a result, RC-active devices are used to simulate inductors on silicon chips. Three basic techniques viz. Riodran's technique, Antoniou's technique and Floating inductor technique for the simulation of an inductor were studied. Simulated inductances were measured experimentally at various frequencies. The circuits were analysed using non-ideal active devices and their performance was calculated. Over the years many methods and techniques have been proposed to simulate positive and negative resistors, inductors and resistively variable capacitors using active devices. Of these, the circuit invented by Antoniou [2] is considered to be among the initial realization of an inductor using actual active devices. This circuit was used in many filter circuits replacing the passive inductor. But this circuit uses two op amps and a number of resistors and a capacitor. A simpler circuit is reported in [3] where two OTAs and a capacitor are used to realize a grounded inductor. Koutzarov in [4] proposes a variable simulated grounded inductance using two amplifiers. The inductance can be controlled digitally or manually, by the gain of one of the amplifiers, while the quality factor

is constant. In [5], Hickman reports how to realize a negative inductor. Moreover, a method to realize negative and positive grounded and floating capacitors is discussed. In [6], a novel ideal grounded inductance simulator (GIS) has been realized using an OTA as the active device. This simulator uses a low component count and has no matching constraint in its implementation. It is linearly tunable over four decades using bias current or voltage control.

In [7], a number of attractive features of second generation current conveyors (CCII) and circuits based on them are discussed. The differences between Op-amps and CCII are outlined. In addition, it is shown how impedance converter and a grounded inductor can be realized using current conveyors. Qiu has suggested in [8] an integrable voltage-controlled simulated inductor with inductance variable from 0.1 to 250,000 H. A method has been proposed in [9] to simulate a voltage controlled inductor using IC four-quadrant analogue multipliers. This avoids the need of many matched transistors required for the circuit balance otherwise. Its features make it suitable for practical applications as a circuit element of a sine-wave oscillator or a filter with linear voltage control characteristics in the low or very-low frequency ranges. A parallel lossless tuned circuit is reported in [10], where the inductor is simulated using two op-amps, four resistors and a capacitor. The circuit can be made to work as a sinusoidal oscillator by connecting a resistor between the non-inverting input of first op-amp and its output.

1.2.2 Negative Impedance Converter (NIC) and Immitance Simulator Circuits

A novel method is proposed in [11] for realizing linear resistors and inductors based on a current inversion-type negative impedance converter (NIC) using MOSFETs in the non-saturation region. In [12], techniques for the electronic tuning of inductors and capacitors, and for the active compensation of their losses and thus the enhancement of their quality factors are discussed. Applications to integrated RLC filters using on-chip inductors are also considered. A new hybrid design approach is proposed in [13] for high quality, high frequency active filters. The idea is based on the active simulation of a classical integrated high frequency transconductance-C inductor but employs optical techniques to achieve the high Q.

It has been shown in [14] that the active-R immitance simulator utilizing a finite gain-bandwidth product gives the reliable high frequency performance. A grounded immitance simulator composed of a single op-amp and thirteen passive circuit elements is presented. Analytical results show that various immitances can be realized. In particular, an increase in the the value of the simulated inductance and the circuit for generating a negative conductance has been discussed. Senani has shown in [15] different methods for the realization of immitances and filters using grounded capacitors and OTAs. The resulting circuits are shown to be superior to those published earlier, and, in addition have features which make them more suitable from the point

of view of IC implementation. In [16], Fabre et al. described a current controlled impedance converter using two translinear active devices: a current conveyor with unity gain and an adjustable differential current-mode amplifier. A CMOS negative impedance converter is presented in [17]. Both current and voltage-controlled negative resistances are available. The circuit operation is based on current and voltage mirroring, providing an overall linear characteristic that is temperature and transistor-insensitive. Pookaiyaudom et al. suggest in [18] that a commercially available dual-operational transconductance amplifier (OTA) package can be efficiently used as both positive and negative second-generation current conveyors, floating negative impedance converters and floating nonlinear impedance converters. In [19], an OTA based wide-tunable-range voltage-controlled resistance converter circuit, where the magnitude of the converted resistance can be electronically varied, is proposed. The circuit is realized through the use of an active network, termed as 'electronically tunable second generation current conveyor' (ECCI). Takagi et al. has proposed in [20], a method for improving the common mode rejection ratio (CMRR) of differential amplifiers by using a balanced-type negative impedance converter. In [21], two configurations are proposed which realize voltage-controlled resistance, inductance and capacitance using op amp and JFET.

1.2.3 Capacitor Simulator Circuits

In [22], a capacitance multiplier circuit, using operational transconductance amplifiers, is realized. The circuit provides wide range linear control of the capacitance value with direct voltage or current. In related developments, Carlosena et al. has proposed a method in [23] to realize a simulated capacitance whose value is controlled by the resistors in the circuit and is called resistively-variable capacitor (RVC). Dunn has reported a circuit in [24] which simulates a variable capacitor whose value can be made positive or negative, depending on the resistor values in the circuit. Using an op amp and an OTA, a variable capacitor is realized in [25] whose value can be made positive or negative. In [26], a new method using negative capacitance is suggested to cancel the input capacitance of instruments and probes.

1.2.4 Operational Transconductance Amplifier (OTA) and Its Circuits

An analogue multiplier with OTAs is presented in [27]. Some attractive techniques have been presented to overcome the typical problems of OTA multipliers: limited input voltage swing and temperature dependence. As a matter of fact these are typical problems of any OTA based circuit and hence these techniques can be applied to any such circuit. In [28] a number of OTA applications in various circuits have been reported. Specifically, applications of the OTA in voltage-controlled amplifiers,

filters and impedance convertors are presented. Advantages and disadvantages and practical limitations of OTA based circuits have also been studied. It has been reported in [29] that OTAs can introduce programmability into any conventional fixed gain circuit. Multipliers, VCAs, VCOs and voltage controlled filters can be easily constructed using OTAs.

It is well known now that OTA circuits having inherent attractive feature of programmability also suffer from some parasitic problems. Some of these problems have been studied and reported. For instance, a unified systematic approach to the design of voltage-controlled oscillators using only operational transconductance amplifiers (OTAs) and capacitors has been discussed in [30]. In addition, the authors have suggested a second-order macromodel of OTA showing its parasitic effects. These include finite input and output impedances, frequency-dependent transconductance gain and output current saturation. Similarly, non-idealities of real CMOS OTAs, including high frequency parasitics have been considered in [31], in order to determine the frequency performance limitations in OTA-C filters. Likewise, Acar et al. have studied in [32] the second-order active filters using a minimum number of OTAs and grounded capacitors, specifically with regard to the limitations on input signal amplitude of OTAs. They derived a simple formula for the input signal amplitude which does not cause clipping and slew-rate-limiting problems.

1.2.5 Current Conveyor (CC) and Its Circuits

The current conveyor, introduced in 1968, is an extremely powerful building block, combining voltage and current-mode capability. It has been proved to be functionally flexible and versatile, rapidly gaining acceptance as a practical device with a wide range of high performance circuit and system applications. A host of circuits have been suggested on the synthesis of various circuit elements using current conveyors [33]. Sedra et al. have given in [34] a historical account of the invention of the current conveyor. Some observations are made on the progress in its realisation and application over the past two decades. New results on the monolithic implementation of the current conveyor are presented. Wilson has discussed the evolution of CCII in [35]. Various old realisations of CCII are reported. A number of applications of the conveyor including gyrators and frequency dependent nagative resistor (FDNR) are described.

1.3 Problem Definition

In the preceding section, it is seen that there are numerous ways of synthesizing a resistor, inductor, or a capacitor using active devices and passive componenets. However, most of these circuits give a fixed value of the simulated component and provide no mean for electronic tunablility in the circuit [1, 14, 23]. Some circuits which do provide this feature using OTAs, suffer from the problem of temperature

dependence of g_m, whose presence renders the overall circuit temperature-dependent [3, 6, 13, 25]. Moreover, very few authors have studied the effect of the non-idealities on the operation of the simulated circuit element.

In order to overcome the problems present in the existing simulator circuits, we shall present, in this thesis, simulator circuits to realise inductor and capacitors such that:

1. The programmable feature of OTAs will be exploited to obtain various voltage/current varibale simulator circuits such that the overall circuits are electronically tunable (digitally programmable)

2. The temperature-dependency introduced due to the addition of an OTA will be dealt in a way to make the overall circuit temperature-independent[1].

3. The stability analysis of some of the simulator circuits will be presented, taking into account the non-idealities in the circuit. This is an essential issue for any simulator circuit, since it sets a limit on its operation and performance as a practical circuit.

In short, the aim of this thesis is to present and discuss a number of Digitally Programmable Temperature-Independent Tuned (DiPTIT) circuits designed and developed during the course of this work.

[1]Independent of V_T

1.4 Thesis Contribution

In order to accomplish the objectives of this thesis, the following steps have been taken:

- Various methods and techniques for realizing tunable simulated components have been discussed and their merits and demerits are investigated.
- Some of the existing circuits, simulating inductors, have been studied and modified to incorporate electronic tunability. In addition, improvement and addition of some new and attractive features such as temperature insensitivity in the circuits have been accomplished.
- Some new circuits, such as temperature-insensitive negative/positive resistively variable, voltage/current controlled capacitor circuits have been developed and tested experimentally. The advantages and disadvantages of these circuits have been reported.
- Two General Impedance Convertor circuits using CCIIs and OTAs have been designed and their function as a temperature-independent voltage/current controlled inductance has been tested successfully.
- The three most important and versatile integrated circuits, viz. operational amplifier, operational transconductance amplifier (OTA) and current conveyor (CCII+) have been used as active devices to synthesize the circuit elements.

- All the newly developed circuits have been tested experimentally either as a voltage divider circuit or a bandpass filter or an oscillator circuit. The calculated and measured values of the simulated components are compared.
- The stability of the op amp based circuits have been studied and reported. In addition, the working range of each circuit is also reported.
- Some suggestions and ideas are presented for future work

1.5 Thesis Organization

The thesis work is organized as follows:

Chapter 1 gives a brief introduction about the tuned circuits and defines the problem. In addition, a detailed literature review is also given. Chapter 2 outlines the different methods and techniques used for the realization of simulated circuit elements, such as general impedance convertor (GIC). It also gives a brief introduction about current conveyors and operational transconductance amplifier; the two widely used active devices for the synthesis of circuit elements.

Chapter 3 deals with the circuits used for the simulation of resistively controlled, voltage/current variable negative and positive capacitors. Chapter 4 discusses various circuits for the realization of simulated inductors, using op-amps, OTAs and CCs. Chapter 5 outlines the stability and the range of the simulated circuit elements, specifically those in which op-amp is used as an active element. Two techniques have

been presented to study the stability of a simulator circuit. Thesis concludes with Chapter 6 giving conclusions and suggestions for future work.

Chapter 2

Simulation of Circuit Elements

2.1 Introduction

The desirablity to reduce the size of the circuits resulted in the integrated circuit (IC) technology. But even after the development of this technology, it was not possible to reduce the size of the circuits employing inductors. In addition, there was always a need to replace a physical component in the circuit with a simulated voltage/current controlled component in order to achieve electronic tunability. Long ago, researchers had developed hypothetical circuits involving dependent current and voltage sources which could realize these simulated circuit elements. Such circuits are classified as General Impedance Convertor (GIC).

As a matter of fact, GIC is an active-RC circuit used to realize (simulate) the operation of a circuit element. For instance, such a circuit may be used to simulate an

inductance, frequency dependent negative resistor (FDNR) or a resistively variable capacitor etc. Moreover, a negative circuit element can be realized. But traditionally GICs have been used to simulate inductors for the active simulation of passive RLC networks [23] because of the fact that the size and cost of the inductor increases as the operating frequencies are lowered. Moreover, it is impossible to fabricate physical inductors using integrated circuit (IC) technology. A large number of realizations are available in literature for grounded and floating circuit elements.

One way to realize a GIC is the use of *gyrator* circuit. In fact, it is the most commonly used active circuit used for the realization of an inductor. It is a two-port network consisting of two voltage-controlled current sources of opposite polarities connected in parallel and back to back.

The realization of an inductor by gyrator is a significant and useful result because, as mentioned before, physical inductors are almost impossible to fabricate using integrated circuit (IC) technology [1].

GICs can also be realized using the nullator-norator (nullor) network which contains two cascaded current-inverting negative impedance convertors (CNICs). Such networks have been used to design GICs for the simulation of inductance and frequency dependent negative resistors (FDNRs) [23].

With the advent of operational amplifier (op-amp) in 1960's it became possible to realize these circuits practically with ICs. Later, the addition of operational transconductance amplifier (OTA) and current conveyor (CC) as active devices

paved the way for the development of even better and improved circuits with very attractive features. In other words, the programmable quality of OTA and the versatility of CC to work both in current-mode as well as voltage-mode, brought about a revolution in GICs.

In the following sections we will discuss briefly about the operation and basics of these two relatively new active devices, since op-amp and circuits based on it are around for quite some time, and it, being the mostly used IC in analog circuits, has its operation and basics very well known. After that we'll revert back to some of GIC circuits, based on these active devices, realizing various circuit elements

2.2 Current Conveyor (CC)

2.2.1 Introduction

Wilson has reported in [35] that over the years electronic engineers seem to have been subconsciously persuaded that the world is voltage dominated; that volts are somehow dominant over amps, and in many cases are far more convenient.

While there are good historical and engineering reasons why this feeling has grown up in the power distribution industry for example, there is less convincing evidence in light-current engineering and electronic circuit design. After all both thermionic valves and transistors may be best regarded as controlled-current components.

However, we quite happily design and assemble both valves and transistors into voltage amplifiers, or reach for a voltage oriented operational amplifier, usually without stopping to think whether using voltage as the controlled parameter is the most appropriate method for the task. We are assisted in this by the fact that manufactures produce a large number of amplifiers whose aim is to produce a controlled voltage output from a voltage input.

Are there good engineering reasons for this or can we in fact build current- mode circuits whose performance is comparable to voltage-mode ones? After all there are advantages to be gained in operating at low impedance levels where stray capacitance would produce shorter time constants and therefore fewer high frequency restrictions [35]. This made the researchers believe that many advantages such as high speeds of processing signals are possible if the signals are in current form.

Current-mode circuits have emerged over the last decade as an important class of analog circuit. There are many advantages gained from a wider view of signal processing embracing current-mode techniques. Furthermore, recent advances in integrated circuit technologies has meant that state-of-the-art analog IC design is now able to exploit the potential of current-mode analog signal processing, providing attractive and elegant solutions for many circuit and system problems.

2.2.2 Definition and Basic Operation

It has been reported in [7] that current conveyors are a combination of voltage and current-mode devices offering low component count and high bandwidth. Unlike op-amps, current conveyors do not have their bandwidth restricted by feedback. They can work over 100 MHz bandwidths and remain stable with both inductive and capacitive loads.

The current conveyor circuits need few additional passive components. Many circuits can be implemented by adding just one or two resistors, so the problems of resistor matching are reduced too. Each element consists of three terminals, X,Y and Z.

There are two classes of CC, viz. first generation current conveyor (CCI) and second generation current conveyor (CCII) as explained subsequently.

2.2.3 First Generation Current Conveyor (CCI)

The operation of this class of CCs can be described by the matrix relationship [33, 34]

$$\begin{bmatrix} i_Y \\ v_X \\ i_Z \end{bmatrix} = \begin{bmatrix} 0 & 1 & 0 \\ 1 & 0 & 0 \\ 0 & 1 & 0 \end{bmatrix} \begin{bmatrix} v_Y \\ i_X \\ v_Z \end{bmatrix}$$

where each variable represent total instantaneous quantities. The operation of CCI can be explained as follows.

Any voltage applied at the Y terminal as v_Y will appear at X independent of the current supplied to X. Thus the circuit exhibits a virtual short circuit at X. Also a current flows through Y equal to the current supplied to X and independent of v_Y. Thus the circuit exhibits a virtual open circuit at Y. Finally, the current supplied to X is conveyed to the output terminal Z where the impedance level is very high.

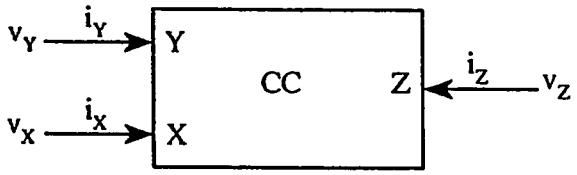

Figure 2.1: Block diagram of current conveyor.

Fig. 2.1 shows a block diagram representation of CCI. For all conveyors the phase relationship between i_X and i_Z is indicated by the algebraic sign in their title, i.e. CCI- or CCI+. By convention positive is taken to mean i_X and i_Z both flowing simultaneously towards or away from the conveyor [34, 35].

Applications of CCI

In [34] it has been reported that an early application for CCI was its use as wideband current measuring device, an alternative to the oscilloscope current probe based on the Hall effect. Although the current meter based on the current conveyor required the measured circuit to be broken to insert terminals X and Y of the conveyor, very impressive results were obtained. Input impedances less than one ohm and a frequency range of operation extending from DC to 100 MHz were measured.

Another early application of CCI was its use as a negative impedance converter (NIC). For this application terminal Z is grounded and the resistor to be converted is connected either between X and ground or between Y and ground.

A major problem that prevented fabrication of the CCI in bipolar IC form in the 1960s is its use of high quality *pnp* devices. However, since complementary devices are available in CMOS technology, it is easy to fabricate a CMOS current conveyor [34].

2.2.4 Second Generation Current Conveyor (CCII)

To increase the versatility of the current conveyor, a second version in which no current flows in terminal Y, was introduced in 1968 [34]. Utilizing the same block diagram of Fig. 2.1, the CCII is described by

$$\begin{bmatrix} i_Y \\ v_X \\ i_Z \end{bmatrix} = \begin{bmatrix} 0 & 0 & 0 \\ 1 & 0 & 0 \\ 0 & \pm 1 & 0 \end{bmatrix} \begin{bmatrix} v_Y \\ i_X \\ v_Z \end{bmatrix}$$

Thus, terminal Y exhibits an infinite impedance. The voltage at X follows that applied to Y, thus X exhibits a zero input impedance. The current supplied to X is conveyed to the high impedance output terminal Z where it is supplied with either positive polarity (in CCII+) or negative polarity (in CCII-).

Applications of CCII

Discussing the applications of CCII, the authors in [34] have stated that its initial application was in the realization of controlled sources, impedance converters, gyrators, and various analog computation elements. Another initial applications included the realizations of a number of nonlinear building blocks that had been previously postulated. Unfortunately, however no widely available circuit realizations for the CCII were given at that time.

Another early realization was the utilization of op-amps and transistor arrays. However, it was realized soon that the op-amp is not the most convenient building block for realizing CCII; the op-amp is fundamentally a voltage-mode device, while the current conveyor is a current-mode device.

Until the past decade or so, few circuit realizations of the CCII have been reported. The situation has changed dramatically with the appearance of a number of good implementations. Some of these utilize IC op-amps together with BJT IC arrays and others utilize CMOS technology, resulting in fully integrated conveyors. It is also interesting to know that several monolithic realizations of the CCII- have been fabricated, although these have been labelled as monolithic nullor elements.

The CCII has proved to be far more useful of the two current conveyor types. The published literature provides CCII realizations for almost all known active network building blocks. A great deal of work has also been reported on the design of active-

RC filters utilizing CCIIs [34].

2.3 Operational Transconductance Amplifier (OTA)

2.3.1 Introduction

Transconductance amplifiers form a useful class of linear IC amplifiers. A transconductance amplifier may also be described as being a voltage-to-current converter (V/I) or voltage-controlled current source (VCCS). It can be shown that a conventional op-amp can be made as a transconductance amplifier; however, monolithic ICs are available that are designed specifically for this purpose. Such devices are called operational transconductance amplifiers, or OTAs.

In the pre-semiconductor days, a figure of merit quoted for electronic valves was the ratio of change of anode current to change of grid voltage. This value was known as mutual conductance (g_m), and allowed the designer to predict the current or voltage gain of a particular circuit. Owing to the prevalence of voltage in, voltage out building blocks, transconductance (now quoted in siemens, S), is only occasionally encountered. This is rather surprising when one considers that transistors are essentially voltage in-current out devices.

In the hybrid-pi model of transistor in common-emitter mode, the base receives an input voltage which the transistor converts to a current at the collector. This current is usually fed into a resistive load, thus giving a voltage output. One can

therefore consider the g_m of a transistor of merit, related to the h_{fe}.

Since the g_m is roughly proportional to the emitter current, it follows that if we supply the emitter current with another voltage to current converter, we have a voltage gain cell. Despite having a limited operating region, this arrangement lends itself to rf modulation when loaded with a tuned circuit to discriminate the desired product.

Extending the transconductance principle a little further yields the operational transconductance amplifier (OTA). In general, OTA is an op-amp whose output current is proportional to the voltage difference between the input pins. An extra pin (I_{set}, I_{bias} or I_{abc}) on OTA chips allows the variation of g_m. An OTA with a resistive load can be considered as an op-amp with open-loop gain, $A_o = g_m R_{load}$.

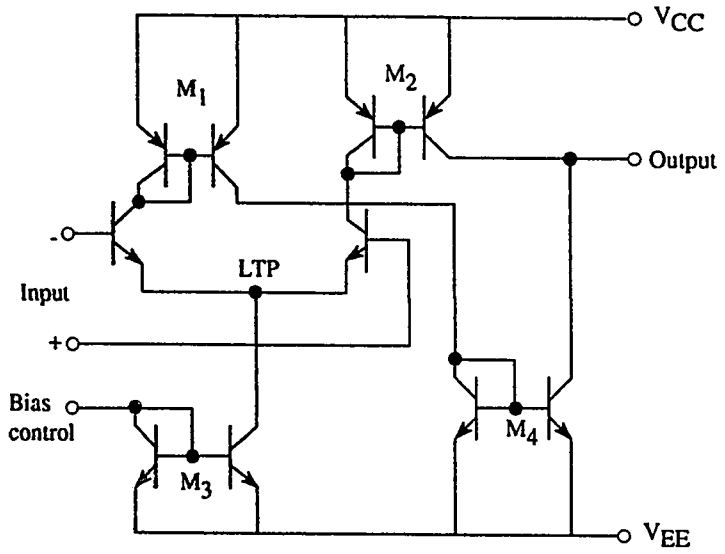

Figure 2.2: Simple operational transconductance amplifier.

Fig. 2.2 reveals how a simple OTA operates. A long tail pair, LTP, provides differential input, as in a conventional bipolar op-amp. Two current mirrors, M_1 and M_2 serve as active loads for the input transistors. Current into M_2 is echoed to the output, whereas the current from M_1 is mirrored again to give a signal ended output. The current from mirror M_3, set by the control input, determines the emitter current of the input pair, and consequently the gain. The symbol and functional diagram of an ideal OTA are shown in Fig. 2.3 (a) and (b) respectively [28, 29].

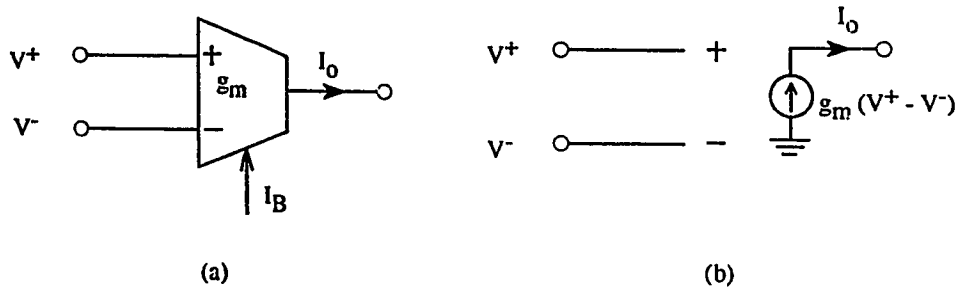

Figure 2.3: Symbol (a) and equivalent circuit of ideal OTA (b).

Transconductance amplifiers form a useful class of linear IC amplifiers. A transconductance amplifier may also be described as being a voltage-to-current converter (V/I) or voltage-controlled current source (VCCS). It can be shown that a conventional op-amp can be made as a transconductance amplifier; however, monolithic ICs are available that are designed specifically for this purpose.

2.3.2 IC Transconductance Amplifiers

The CA3080 owes its longevity to simple but versatile design. Devices such as LM 13600 and LM 13700 have significantly better specifications. The internal circuitry of the CA3080 differs only a little from that of Fig. 2.2 and adds a significant harmonic distortion to signals above a few tens of a millivolt [29].

Low distortion from the CA3080 is usually achieved by attenuating the signal before the device and using subsequent stages to restore the amplitude [27, 28, 29, 32]. This distortion/dynamic range problem has been partially tackled in the LM13600 which has a diode network to linearize the chip's response for larger signals. The device also includes two darlington pairs whose collectors are internally connected to the positive supply pin. These can act as buffers or play more active role in circuits as separate gain elements.

2.3.3 Practical Applications

Since the output of an OTA is current, hence it can be used very well in circuits involving signal summing. One can simply wire the outputs of separate devices together to share the same load. The summing and gain control capabilities of OTAs are perfect for the core of a multiplexer, where applying a current to the appropriate g_m control pin, selects one of several inputs. The CA3080 has an extra benefit here; its standby power demand is only 10μW.

The 50V/μs slew rate of OTAs make them usable for high frequency amplification and switching applications. The current output also simplifies impedance matching to cables, as the OTA load is the output impedance. In addition, OTAs find application in a host of circuits such as voltage controlled amplifier (VCA), automatic gain control (AGC), voltage controlled resistors, voltage controlled filters, voltage controlled oscillators, general impedance converters (GICs) for the simulation of circuit elements [27, 28, 29, 32].

2.4 A Remark Regarding the Value of g_m of an OTA

It is well known that the transconductace gain of an OTA, g_m, is expressed as

$$g_m = \frac{I_B}{2V_T} \tag{2.1}$$

where I_B is the amplifier bias current and V_T is the thermal volatge.

However, during the course of this work, it was found that a better and more accurate expression for g_m should be

$$g_m \approx \frac{I_B}{2V_T} \tag{2.2}$$

The need for this expression arised because it was observed while performing experiments on some OTA based circuits that the discrepeny in theoretical and experimental results was high even if temperature-dependency is taken into account. This

high value of discrepency could be attributed to imperfection of current-mirrors and other non-idealitites in the OTA circuit.

Subsequently, we will present some general impedance converter circuits based on the active elements discussed above.

2.5 Some General Impedance Converter Circuits

Fig. 2.4 shows a single op-amp based GIC, with three passive circuit elements only. The input impedance, Z_{in}, of the circuit is calculated as follows.

Assuming ideal op-amp, the two inputs of the op-amp are virtual short circuit, and hence the voltage at the inverting input is also v. Therefore, output voltage v_o is given by

$$v_o = (1 + \frac{Z_2}{Z_1})v$$

Now the current i is given by

$$i = \frac{v - v_o}{Z_3}$$

Substituting the value of of v_o gives

$$\frac{i}{v} = \frac{1 - (1 + \frac{Z_2}{Z_1})}{Z_3}$$

which gives the input impedance, Z_{in} as

$$Z_{in} = \frac{v}{i} = -\frac{Z_1 Z_3}{Z_2} \tag{2.3}$$

The circuit can be used to simulate a voltage/current controlled negative/positive inductance, resistance or a resistively controlled capacitance.

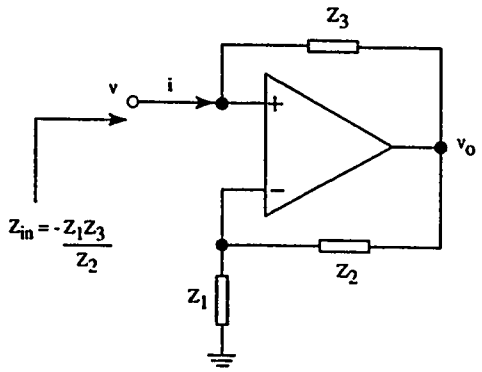

Figure 2.4: An op-amp based general impedance convertor.

Fig. 2.5 shows another GIC circuit designed during the course of this work. The circuit uses OTAs and op-amp. The input impedance, Z_{in}, is given by

$$Z_{in} = Z_7 \parallel \frac{Z_5 Z_7}{g_{m1} g_{m3} Z_2 Z_4 Z_6}$$

The circuit can simulate various circuit elements. Its application as temeprature-independent voltage variable inductor will be described in chapter 4.

The GIC shown in Fig. 2.6 is a CCII based, all grounded component circuit. The input impedance, Z_{in}, of the circuit is given by

$$Z_{in} = -\frac{Z_1 Z_3}{Z_2}$$

The realization of a fixed inductor using this GIC has been reported [7]. However, this circuit can be used to realize a voltage/current variable inductor, as discussed

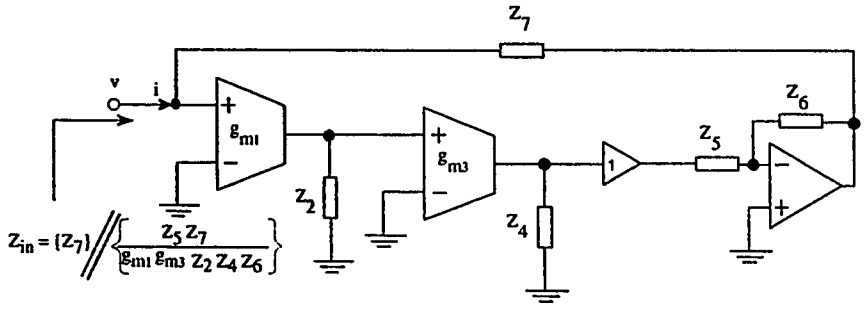

Figure 2.5: OTAs and op-amp based GIC.

in chapter 4. Moreover, the circuit can be used to synthesize other circuit elements, such as frequency dependent negative resistor (FDNR) and voltage variable capacitor.

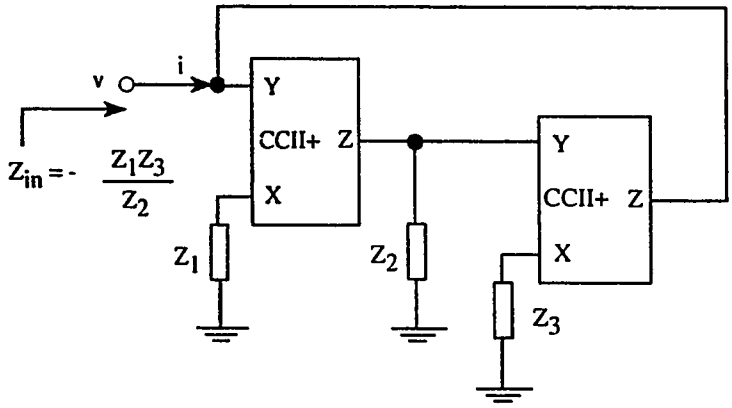

Figure 2.6: An all grounded component GIC employing two CCIIs.

The above circuit can be extended to obtain a more versatile circuit shown in Fig. 2.7 [36]. The input impedance, Z_{in}, of this circuit is given by

$$Z_{in} = -\frac{Z_1 Z_3 Z_5}{Z_2 Z_4}$$

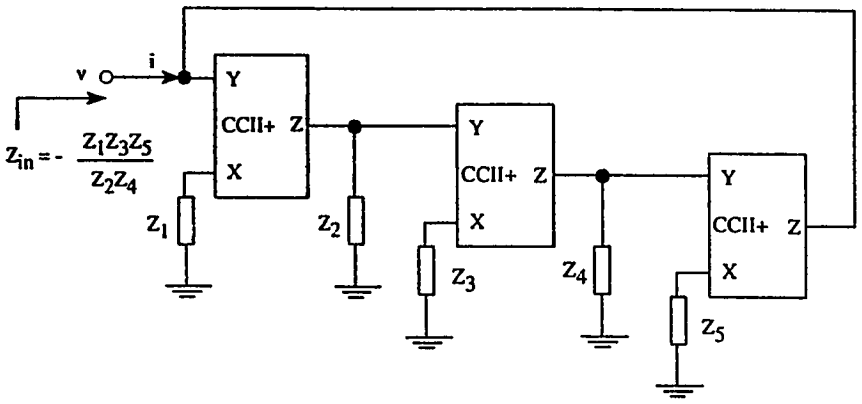

Figure 2.7: An all grounded component GIC employing three CCIIs.

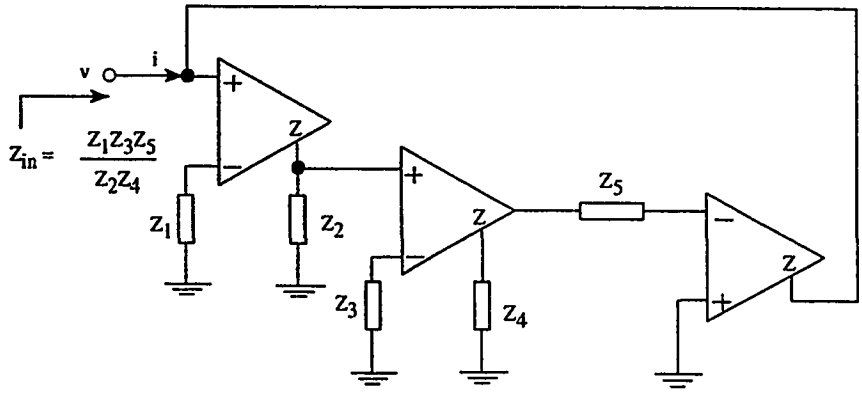

Figure 2.8: A GIC employing AD844 ICs.

A variety of circuits can be realized using this circuit. A temperature-independent, voltage/current controlled inductor has been realized using this circuit which will be discussed in chapter 4.

The negative sign in the expression for the input impedance can be got rid of, at the cost of having one floating component in the circuit, by using a current feedback amplifier such as AD844, as shown in Fig. 2.8.

Some applications of these GICs for the realization of different circuit elements will be discussed in subsequent chapters.

Chapter 3

Simulated Capacitance Circuits

3.1 Introduction

Over the years many attempts have been made to realize circuits using active devices, one or more capacitors and a few resistors such that the input impedance of the circuit simulates a capacitor whose value may depend on resistors or some other parameters in the circuit. By varying these parameters the value of the simulated capacitor can be increased or decreased [22, 23, 24, 25]. Most of these circuits are based on the Miller effect, i.e. if a capacitor is connected between two nodes 1 and 2 such that node 2 is at higher potential than node 1 (voltage at node 2 should be independent of the connection of this capacitor), then the circuit will simulate a capacitor between node 1 and ground. If the voltage at node 2 is in phase with that at node 1, then the simulated capacitor will be negative, otherwise positive. The

same idea can be used for the simulation of negative resistor.

There is always a need of such circuits from the IC implementation point of view, since a capacitor requires a large area on chip. Using this technique, a small capacitor can be made to work as a large capacitor effectively. In addition, such circuits also find application in discrete tuned circuits.

In some cases, the value of the simulated capacitor depends on the resistors in the circuit. Replacing these resistors by OTA connected resistors, brings electronic tunability into the circuit, since the resistance of these OTA resistors can be varied by varying the bias voltage/current of the OTA. This is a very attractive and useful feature if the circuit is to be digitally controlled.

In the following sections we will present three simple OTA circuits which realize, voltage controlled grounded positive resistor, voltage controlled grounded negative resistor, voltage controlled floating (neither of the two ends of the resistor are grounded) positive resistor. All these simulated resistors can be varied by a varying the bias voltage/current of the OTA(s). They will be used extensively in this thesis work, to achieve electronic tunability in other simulated circuit elements.

3.1.1 OTA Connected Grounded Positive Resistor

Consider the OTA circuit shown in Fig. 3.1 [28].

The output current of the OTA is $g_m v$, which is the same as i. Therefore, the

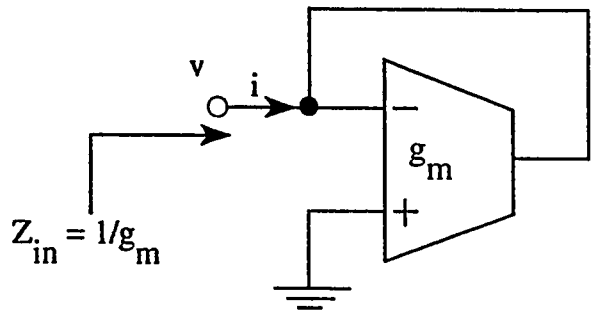

Figure 3.1: Grounded postive resistor realized using an OTA.

input impedance is given by

$$Z_{in} = \frac{v}{i} = \frac{1}{g_m}$$

which is equivalent to a resistor, R_{eq}. Thus

$$R_{eq} = \frac{1}{g_m}$$

is a simulated, positive, grounded resistor. g_m is the transconductance of the OTA whose value is given by

$$g_m = \frac{I_B}{2V_T}$$

where I_B is the amplifier bias current and V_T is the thermal voltage whose value is 26 mV at 27°C. Therefore, the g_m and hence R_{eq} can be changed by changing biasing voltage/current of the OTA which makes the circuit electronically tunable.

3.1.2 OTA Connected Grounded Negative Resistor

Consider the OTA circuit shown in Fig. 3.2 [30].

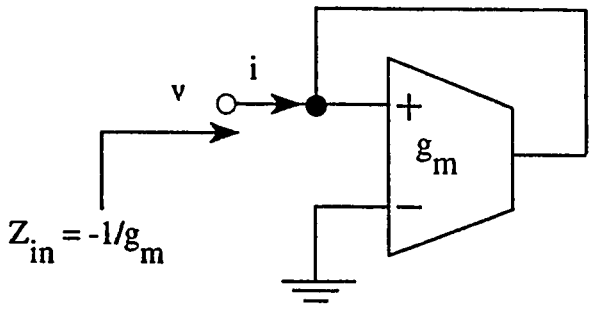

Figure 3.2: Grounded negative resistor realized using an OTA.

The output current of the OTA is $g_m v$, which is related to i as

$$i = -g_m v$$

Therefore, the input impedance is given by

$$Z_{in} = \frac{v}{i} = -\frac{1}{g_m}$$

which is equivalent to a negative resistor, R_{eq}. Thus

$$R_{eq} = -\frac{1}{g_m}$$

is a simulated, negative, grounded resistor.

3.1.3 OTA Connected Floating Resistor

Refer to the two OTAs (A & B)circuit shown in Fig. 3.3 [28]. Assume that the two OTAs are biased by the same currents such that they have the same g_m.

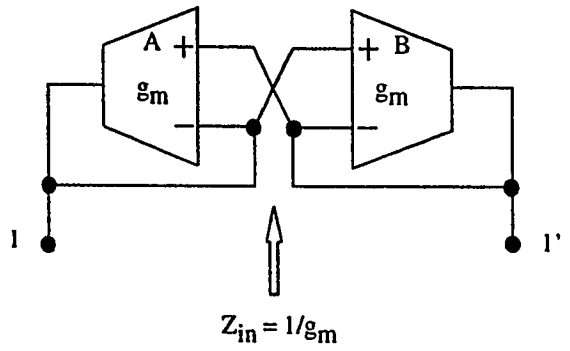

Figure 3.3: Floating resistor realized using two OTAs.

Let us suppose that a voltage v is applied between terminals 1 and 1', such that a voltage $v/2$ appears at node 1 and -$v/2$ at node 1' respectively, with respect to ground. Let the current flowing into the terminal 1 be i_+ and the current coming out of terminal 1' be i_-. The output current of OTA A is -$g_m v$. This current is the same as i_+. i.e. $i_+ = g_m v$. Similarly, $i_- = g_m v$. This situation can be represented by the equivalent circuit shown in Fig. 3.4. Now since $i_+ = i_- = i$, therefore,

$$Z_{in} = \frac{v/2 - (-v/2)}{i} = \frac{v}{g_m v}$$

Thus the input impedance of this circuit is equivalent to a resistor, R_{eq} given by

$$R_{eq} = \frac{1}{g_m}$$

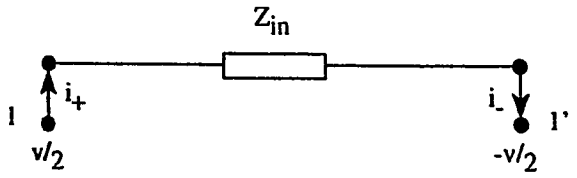

Figure 3.4: The equivalent circuit of OTA connected floating resistor.

In the subsequent sections, a few simulated capacitor circuits developed employing the above mentioned voltage/current controlled resistor circuits will be discussed.

3.2 Grounded Positive Capacitor

In chapter 2, it was shown that the input impedance for the general impedance convertor (GIC) shown in Fig. 2.4 is given by

$$Z_{in} = -\frac{Z_1 Z_3}{Z_2}$$

Let us consider the case when $Z_1 = R_1$, $Z_2 = R_2$ and $Z_1 = \frac{1}{C_3 s}$. The input impedance becomes

$$Z_{in} = -\frac{R_1}{R_2 C_3 s}$$

which is equivalent to a capacitor, C_{eq}, given by

$$C_{eq} = -\frac{R_2 C_3}{R_1}$$

Thus a negative, resistively controlled grounded capacitor is simulated [37]. The value of negative capacitance can be varied (tuned) by varying R_2 or R_1 or both. In

order to introduce electronic tunability in the circuit, R_1 could be replaced by OTA connected resistor (note that replacing R_2 will require two OTAs) as shown in Fig. 3.1 or Fig. 3.2. In order to obtain a positive simulated capacitor, the OTA circuit of Fig. 3.2 will be used. Thus C_{eq} becomes

$$C_{eq} = g_{m1} R_2 C_3 \tag{3.1}$$

As mentioned in Chapter 2, we will use the expression for g_{m1} as the one given in Equation 2.2, i.e.

$$g_{m1} \approx \frac{I_{B1}}{2V_T}$$

where, as mentioned before, I_{B1} is the bias current of OTA, V_T is the thermal voltage. The resulting circuit though electronically tunable will be temperature dependent and will give unreliable results because of the reasons mentioned in Chapter 2. Thus the use of Equation 2.2 as such is not very desirable. In order to make the circuit temperature-insensitive, and get more accurate results, R_2 is replaced by the floating resistor of Fig. 3.3 to make the expression for C_{eq} as

$$C_{eq} = \frac{I_{B1}}{I_{B2}} C_3$$

Therefore C_{eq} is a temperature-independent[1], voltage/current controlled grounded, positive capacitor.

[1]Independent of V_T

3.2.1 Experimental Results

The circuit used to test this simulated capacitor is shown in Fig. 3.5.

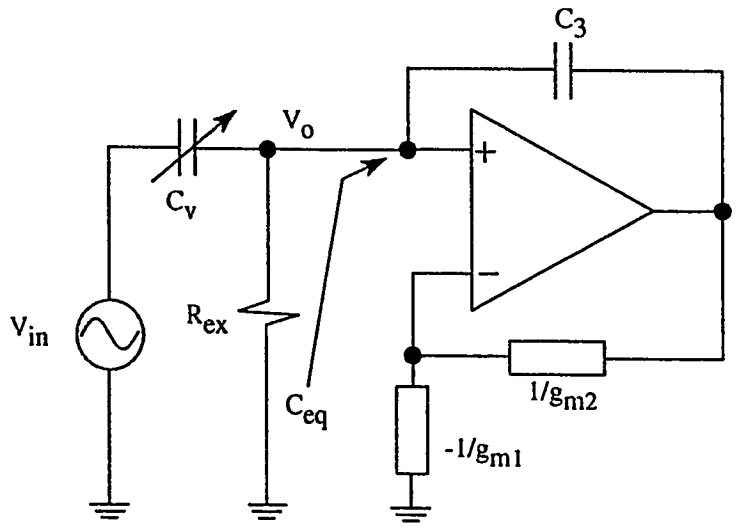

Figure 3.5: Circuit used for testing the simulated positive capacitor.

The circuit consists of an external capacitor, C_v connected in series with the simulated capacitor, C_{eq}, to form a voltage divider network. A resistor R_{ex} of 220KΩ was connected to provide a path to the bias current, to ground. The input was a sinusoidal signal of 1 KHz, with an amplitude of 40 mV peak. The bias current, I_{B2} was fixed at 30.8 μA. C was a 1μF capacitor, while C_{ex} was a decade capacitor box. CA741 op-amp was used and LM13600 OTA chips were used.

Table 3.1 shows the measured and calculated values of the simulated capacitor, C_{eq} as the other bias current, I_{B1} is varied. Fig. 3.6 shows the graphs of calculated

and measured C_{eq} versus I_{B1} which are in close agreement, except at relatively large values of I_{B1}.

The range of the simulated capacitor is limited by the non-idealities in the circuit, specifically, those of op-amp. The circuit tends to distort the signal as the value of simulated capacitance is reduced lower than $30n$F and shows instability, as C_{eq} is increased beyond $620n$F. The stability of some op-amp based simulator circuit will be discussed in Chapter 5.

I_{B1} (μA)	C_{eq}(measured) (nF)	C_{eq}(calculated) (nF)	% error (%)
1.0	30	32	6.25
5.0	160	162	1.23
10.0	300	320	6.25
15.0	460	490	6.12
20.0	620	650	4.61

Table 3.1: Table comparing measured and calculated values of C_{eq}.

3.3 Grounded Negative Capacitor

In the preceding section, if resistor R_1 is replaced by the OTA circuit of Fig. 3.1, the value of C_{eq} becomes

$$C_{eq} = -\frac{g_{m2}}{g_{m1}} C_3$$

or

$$C_{eq} = -\frac{I_{B1}}{I_{B2}} C_3$$

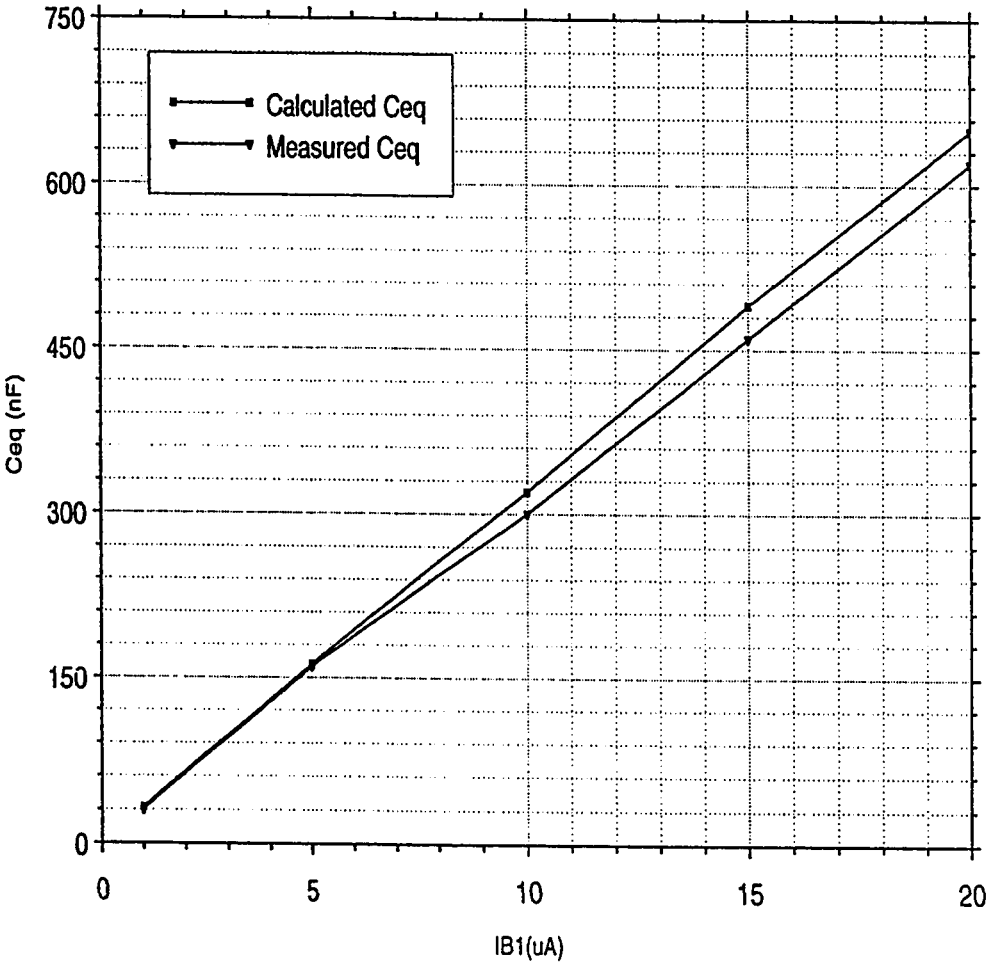

Figure 3.6: Graph between C_{eq} and I_{B1}.

Therefore C_{eq} is a temperature-independent[2], voltage/current controlled grounded, negative capacitor. In order to get a positive value of capacitance from this circuit, an external capacitor, C_{ex} should be connected between the non-inverting input of the op-amp and ground, such that the value of the simulated negative capacitance must not exceed this external capacitor. In that case, the equivalent capacitance, $C_{eq'}$ is given by

$$C_{eq'} = C_{ex} - \frac{I_{B1}}{I_{B2}} C_3$$

3.3.1 Experimental Results

Fig. 3.7 shows the configuration alongwith the values of the components used for measurements.

I_{B2} was fixed at 14.7μA. I_{B1} was varied to get different values of $C_{eq'}$, as shown in Table 3.2.

The graph between the measured and calculated values of $C_{eq'}$ is shown in Fig. 3.8. It is clear from the graph and Table 3.2 that the calculated and measured results are in close agreement with I_{B1} values less than equal to 12μA, corresponding to $C_{eq'}$ values of about 700nF to 1μF. As the value of I_{B1} was increased beyond 24μA, the output of the circuit shown in Fig. 3.7 became distorted and showed signs of instability. This is due to the non-idealities of the op-amp and OTAs, specifically in this case the limited differential input voltage swing of OTAs poses serious problem

[2]Independent of V_T

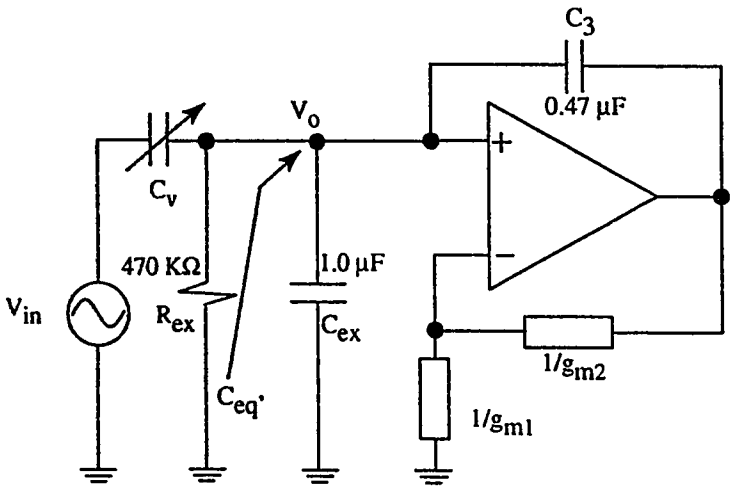

Figure 3.7: Circuit used for testing the simulated, negative capacitor.

I_{B1} (μA)	$C_{eq'}$(measured) (nF)	$C_{eq'}$(calculated) (nF)	% error (%)
0	1000	1000	0
3.3	900	890	1.12
7.0	800	780	2.56
12.0	700	620	12.90
17.0	600	460	30.43
21.3	500	320	56.25
24.0	430	230	86.96

Table 3.2: Table comparing measured and calculated values of $C_{eq'}$.

as the value of the simulated capacitance is increased. This is explained below.

The maximum input differential swing of the LM13600 OTAs used in these experiments was found to be about $50mV$. As the value of the simulated capacitance is increased by increasing R_2, v_o in the circuit of Fig. 2.4 increases. As mentioned before, R_2 is being simulated by two OTAs ($\frac{1}{g_{m2}}$), therefore, one input of each of the two OTAs is at input voltage v, while the other is at v_o. Therefore, there is maximum value of v_o that could be attained, which sets a limit on the maximum value of the simulated capacitance which could be obtained from the circuit.

The instability of the simulator circuits due to op-amp non-idealities will be discussed in chapter 5.

In order to overcome the problem of limited input swing of the OTAs, the following scheme was tried.

3.4 Grounded Negative Capacitor With Buffer

The circuit shown in Fig. 3.9 is used to minimize the effect of input voltage swing of OTAs. The circuit is analysed as follows.

The voltages v_x and v are given by

$$v_x = (\frac{R_3}{R_3 + R_4})v_o$$

$$v = (\frac{R_1}{R_1 + R_2})v_x$$

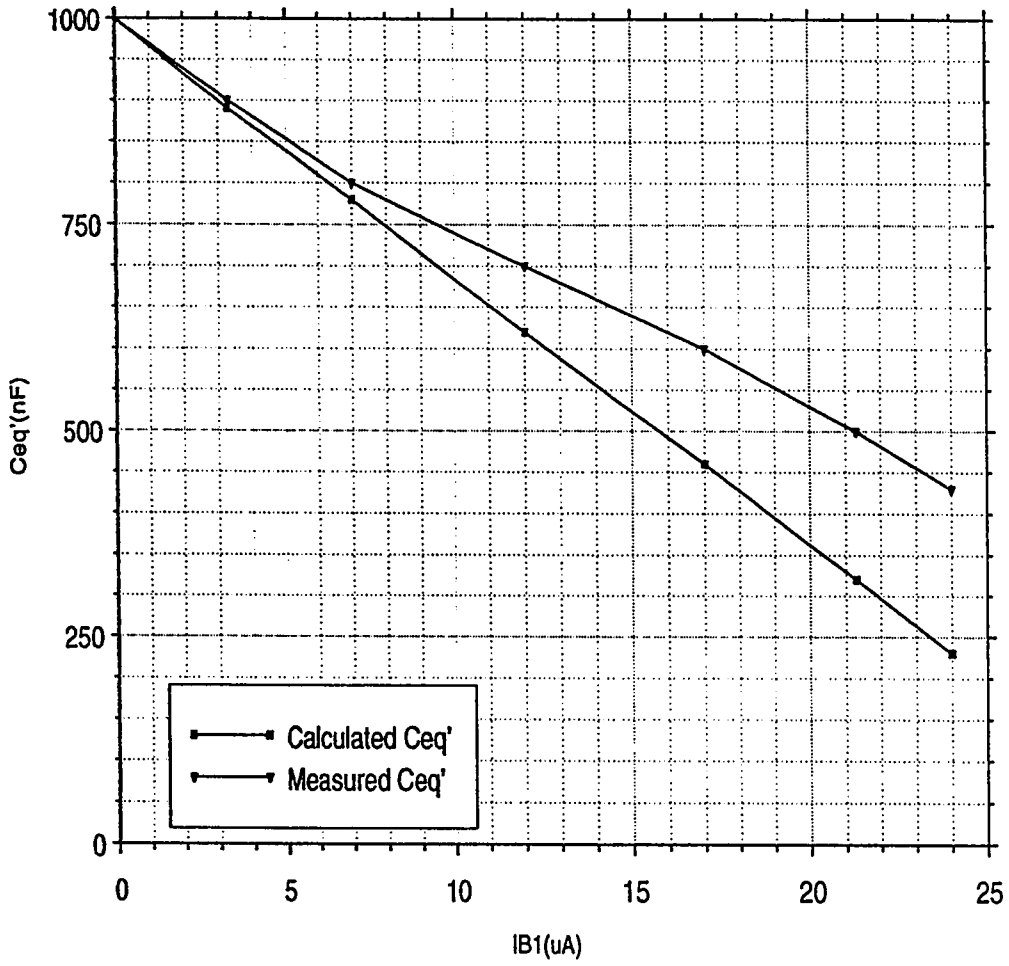

Figure 3.8: Graph between $C_{eq'}$ and I_{B1}.

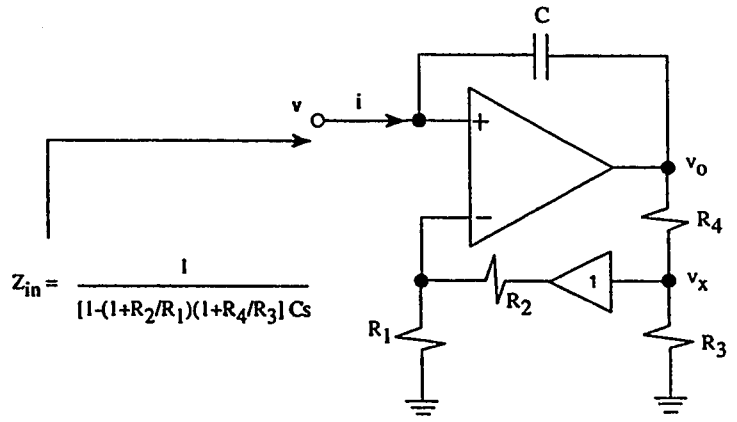

Figure 3.9: The circuit used to minimize the input swing of OTAs.

Therefore,

$$v_o = (1 + \frac{R_2}{R_1})(1 + \frac{R_4}{R_3})v$$

and as described before, using OTAs, it is simple to show that simulated capacitance, C_{eq} is given by

$$C_{eq} = [1 - (1 + \frac{I_{B1}}{I_{B2}})(1 + \frac{R_4}{R_3})]C$$

To get a positive capacitance out of this circuit a capacitor, C_{ex} is added externally in parallel to this simulated capacitor. Thus the resultant positive capacitor, $C_{eq'}$ is given by

$$C_{eq'} = C_{ex} + C_{eq}$$

3.4.1 Experimental Results

The circuit used to verify this idea experimentally is similar to that shown in Fig. 3.7, except that C_{eq} is obtained from circuit shown in Fig. 3.9. The values of the components used were as follows. $R_3 = 1.2\text{K}\Omega$, $R_4 = 2.2\text{K}\Omega$, $C = 0.47\mu\text{F}$. Buffer used is the one available inside LM13600 dual OTA chip. I_{B2} was fixed at $14.7\mu\text{A}$. I_{B1} was varied to get different values of $C_{eq'}$, as shown in Table 3.3.

I_{B1} (μA)	$C_{eq'}$(measured) (nF)	$C_{eq'}$(calculated) (nF)	% error (%)
0	800	740	8.11
0.5	700	720	2.78
3.0	600	590	1.70
5.0	500	490	2.04
6.5	400	420	4.76
7.7	300	360	16.67
9.8	200	260	23.10

Table 3.3: Table comparing measured and calculated values of $C_{eq'}$.

The graph between the measured and calculated values of $C_{eq'}$ is shown in Fig. 3.10. It is obvious from Table 3.3 and graph of Fig. 3.10 that there is not an appreciable increase in the range of the simulated capacitance as compared to the one discussed in the previous section. This is so because the addition of R_3 and R_4, in fact, result in an increase in v_o by a factor of $(1 + \frac{R_1}{R_3})$. Thus, the voltage at v_x remains the same as in the previous case. But still, we do get something out of this circuit! Table 3.3 and Fig. 3.10 indicate that the circuit works well

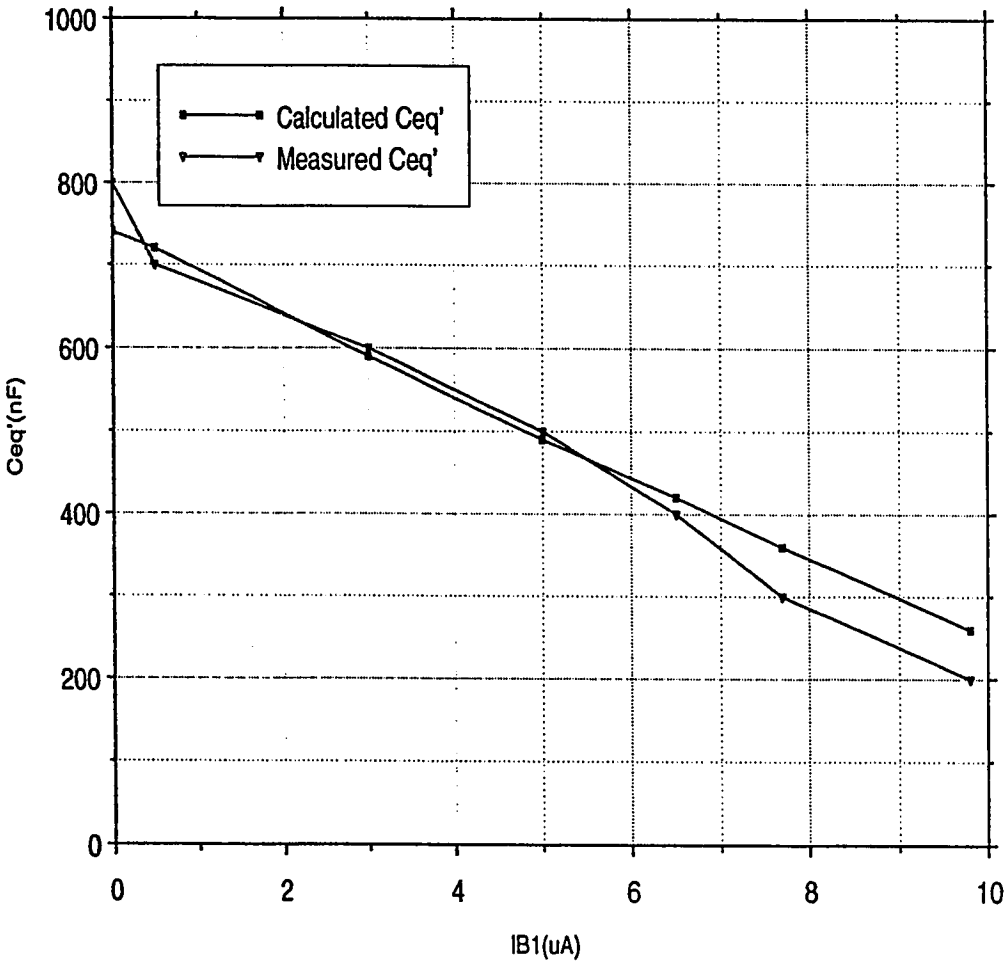

Figure 3.10: Graph between $C_{eq'}$ and I_{B1}.

for I_{B1} values less than equal to 8μA, corresponding to $C_{eq'}$ values of about $300n$F to $800n$F. Comparing these results with those obtained in the preceding section it can be concluded that this circuit simulates relatively large range of capacitance values as compared to the previous one. Moreover, small variations in I_{B1} in this circuit, simulate almost the same range of the capacitance, as realized by the circuit of preceding section.

Chapter 4

Simulated Inductance Circuits

4.1 Introduction

Kumar et al. have given a detailed account of inductor simulation circuits in [1]. They stated that the recent trends in electronics has been toward reducing the size of circuits; a trend which culminated in the development of integrated circuits. Although it is relatively easy to reduce the dimensions of resistors and capacitors it is impractical to do so for inductors. The important reasons for this are the following:

- Semiconductors, which provide the building material of integrated circuits, do not exhibit ferromagnetism. Hence, both the magnetic material forming the core and the conductors forming the windings of the inductor must be deposited on the semiconductor surface. This arrangement results in inductors

of very low inductance L and poor quality factor Q.

- The inherent relation between the physical size of an inductor and its quality factor creates a size problem. If the size of inductor is reduced by replacing every linear dimension 1 by x, then a new quality factor Q_n will become x^2Q, where Q is the original quality factor. Thus, reduction in size of inductor reduces the quality factor greatly.

- Even large inductors are quite lossy. The best attainable Q_L is about 1,000; by contrast, capacitors with Q_c values of 5,000 to 10,000 can be obtained.

- For frequencies below 20 Hz for example, the size and weight of inductors become exceedingly large and Q_L becomes very low. Hence, inductors are seldom used at such low frequencies.

- Inductors using ferromagnetic materials are basically nonlinear elements. Hence, unless the amplitude of the signal which they handle is kept small and direct currents are avoided, they generate harmonic distortion.

- Inductors tend to act as small antennas, radiating as well as picking up electromagnetic waves. This can result in undesirable noise and coupling of signals in circuits containing inductors.

Thus, conventional wire-wound inductors are bulky and costly. There also exists fundamental limitations on the realization of inductances for microminiature and

integrated circuit applications. As a result, there has been increasing interest in the realization of active RC filters requiring no inductance. The advantages in using active RC filters are the reduction in size, weight, cost, and power consumption, and an increase in the system reliability in comparison to discrete versions.

There have been three distinct techniques of inductance simulation

- Active R utilizing the frequency sensitive properties of an op-amp
- Active RC in which the op-amp is modeled by controlled sources with real parameters and resistances
- Techniques based on mechanical resonance in piezoelectric materials.

Active R methods are usually associated with serious stability and sensitivity problems and the amount of success achieved with the mechanical resonance method appears to be very limited. An active RC circuit is most useful and is widely used for replacing inductances in an LC-resistively terminated network. Such an active RC is expected to have as low a sensitivity as a passive circuit, except for imperfections in the realization of active inductors [1].

The most commonly used active circuits for the realization of inductor are called general impedance converters (GICs). Various GIC circuits were discussed in Chapter 2 and in the subsequent sections, it will be shown how to realize inductors using them. It should be pointed out here that the OTAs used in all the following configurations were LM13600.

4.2 Two Op-amp Based Grounded Inductor

McKenny has discussed a scheme in [10] to realize a grounded inductor and showed that its value is R^2C. This circuit has been redrawn in Fig. 4.1 such that all the resistors are given different symbols.

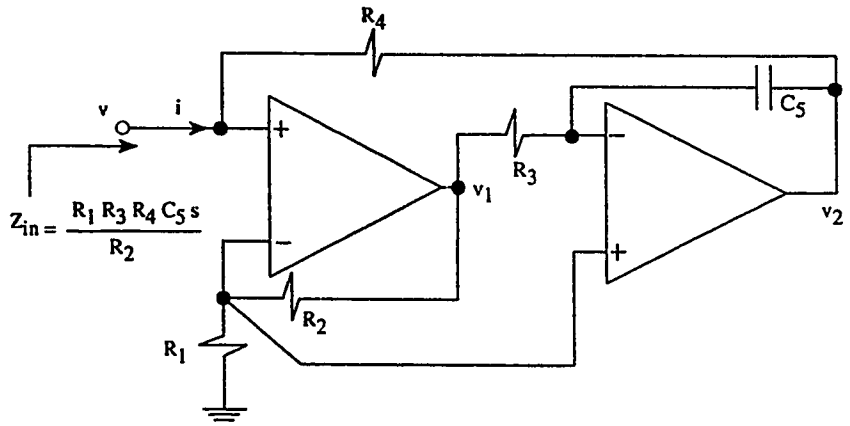

Figure 4.1: Two op-amp based inductor.

Referring to this figure, voltage v_1 is given by

$$v_1 = (1 + \frac{R_2}{R_1})v$$

and the voltage v_2 is

$$v_2 = (1 + \frac{1}{R_3C_5s})v - (\frac{1}{R_3C_5s})v_1$$

Substituting the value of v_1 in the above equation gives,

$$v_2 = (1 + \frac{1}{R_3C_5s})v - (\frac{1}{R_3C_5s})(1 + \frac{1}{R_3C_5s})v$$

or

$$v_2 = v - (\frac{R_2}{R_1 R_3 C_5 s})v$$

Now

$$i = \frac{v - v_2}{R_4}$$

which gives the input impedance, Z_{in} as

$$Z_{in} = \frac{v}{i} = \frac{R_1 R_3 R_4 C_5 s}{R_2}$$

This is equivalent to an inductor, L_{eq} given by

$$L_{eq} = \frac{R_1 R_3 R_4 C_5}{R_2}$$

Thus L_{eq} is a lossless, grounded inductor. This inductor can be made tunable by replacing one of the four resistors by OTA connected resistors of Chapter 3. Replacing R_1 by a single OTA connected resistor ($\frac{1}{g_{m1}}$), would be a better choice, since replacement of any other will require two OTAs. This will yield an electronically tunable grounded inductor. However, as mentioned in Chapter 3, the introduction of OTA will also make the circuit temperature-dependent and unreliable. To overcome this problem, as has been done previously, R_2 is also replaced by a floating OTA resistor ($\frac{1}{g_{m2}}$). Thus the value of the simulated inductor, L_{eq}, becomes

$$L_{eq} = \frac{I_{B2} R_3 R_4 C_5}{I_{B1}}$$

which is a lossless, temperature-independent[1], voltage/current controlled grounded inductor.

[1]Independent of V_T

4.2.1 Experimental Results

To verify the operation of the simulated inductor, the parallel tuned circuit shown in Fig. 4.2 was used.

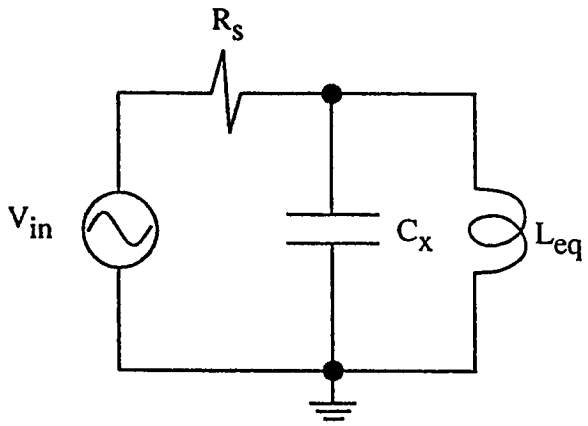

Figure 4.2: Tuned circuit to verify the operation of simulated inductor.

Following values of the components were used. $R_s = 1\text{M}\Omega$, $R_3 = R_4 = R = 200\Omega$, $C_x = C_5 = C = 0.1\mu\text{F}$. I_{B2} was fixed at $31.1\mu\text{A}$ and CA741 op-amps were used. I_{B1} was varied to vary the simulated inductance. For each value of the simulated inductance, the corresponding resonance frequency, f_r, given by

$$f_r = \frac{1}{2\pi\sqrt{L_{eq}C_x}}$$

or

$$f_r = (\frac{1}{2\pi RC})(\sqrt{\frac{I_{B1}}{I_{B2}}})$$

was recorded and used to compute the measured value of L_{eq} as

$$L_{eq}(measured) = \frac{1}{4\pi^2 {f_r}^2 C}$$

or

$$L_{eq}(measured) = \frac{0.2533}{{f_r}^2}\text{H}$$

(where the "mega" part of ${f_r}^2$ (10^6) has already been taken into account in the above expression) while the theoretical value was computed using

$$L_{eq}(calculated) = \frac{0.1244}{I_{B1}}\text{H}$$

(where the "micro" part of I_{B1} (10^{-6}) has already been taken into account in the above expression)

Table 4.1 shows the experimental and calculated results as a function of I_{B1}. It also gives percentage error between the measured and calculated results. The same data is depicted in the form of a graph, shown in Fig. 4.3.

It was observed that for values of I_{B1} less than equal to 1.5μA, the output voltage was distorted and for values around 55μA, the circuit showed the tendency to oscillate. Moreover, due to relatively large percentage error at low values of I_{B1}, it is recommended not to operate the circuit for low values of I_{B1} (less than 1.5μA). The stability of the circuit will be discussed in Chapter 5.

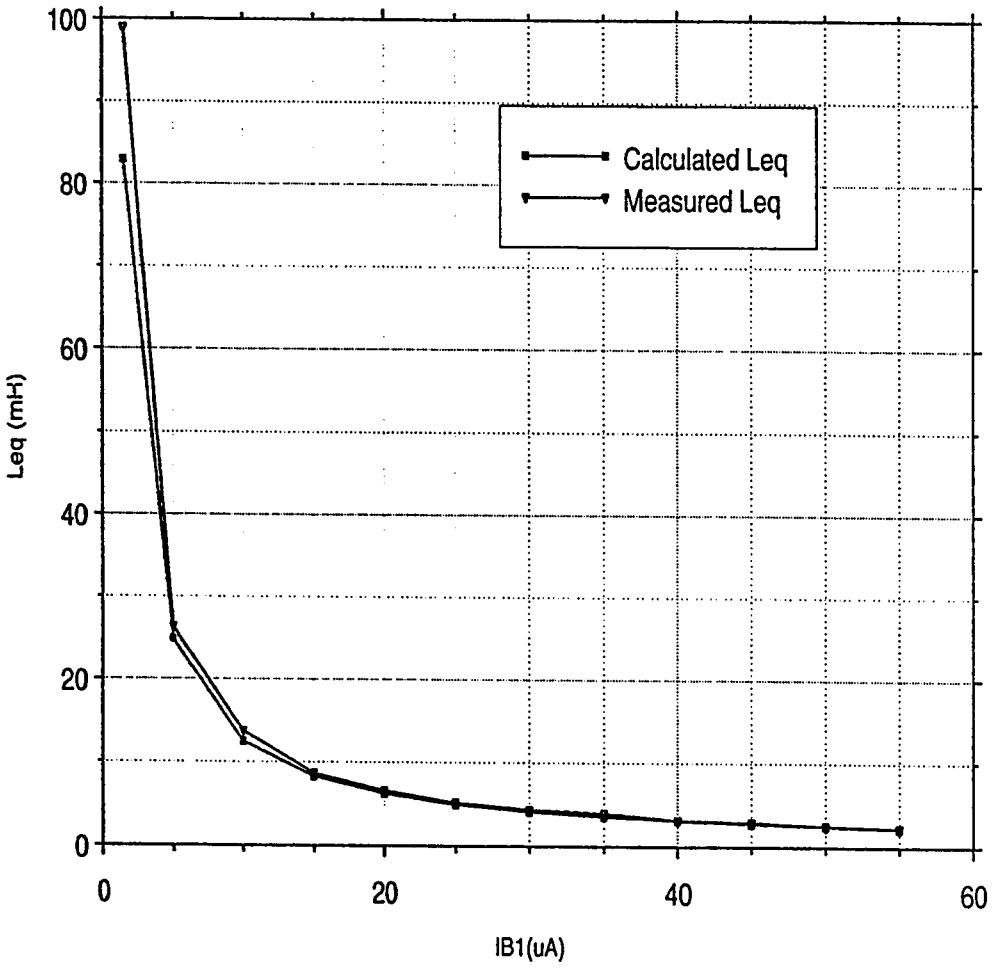

Figure 4.3: Graph between L_{eq} and I_{B1} for the two op-amp based inductor.

I_{B1} (μA)	L_{eq}(measured) (mH)	L_{eq}(calculated) (mH)	% error (%)
1.5	98.95	82.93	19.32
5.0	26.36	24.88	5.95
10.0	13.70	12.44	10.13
15.0	8.68	8.29	4.70
20.0	6.60	6.22	6.10
25.0	5.17	4.98	3.80
30.0	4.38	4.15	5.50
35.0	3.96	3.55	11.55
40.0	3.13	3.11	0.64
45.0	2.93	2.76	6.16
50.0	2.46	2.49	1.20
55.0	2.24	2.26	0.90

Table 4.1: Comparison of measured and calculated values of L_{eq}, for the two op-amp based inductor.

4.3 OTA Based Temperature-Dependent Inductor

Sellani in [3] has presented a very simple circuit containing only two OTAs and one capacitor to realize a grounded inductor. This circuit is shown in Fig. 4.4.

A simple analysis of the circuit shows that the input impedance of the circuit is given by

$$Z_{in} = \frac{C_2 s}{g_{m1} g_{m3}} \tag{4.1}$$

which is equivalent to an inductor, L_{eq}, given by

$$L_{eq} = \frac{C_2}{g_{m1} g_{m3}}$$

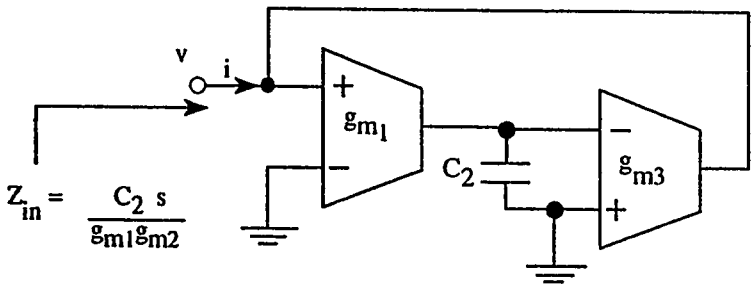

Figure 4.4: A simple but temperature-sensitive inductor circuit.

Thus we have realized a tunable, lossless grounded inductor. Apart from the attractive feature of being electronically tunable, the circuit suffers severely from the drawback of being highly temperature-dependent, since two temperature-dependent terms g_{m1} and g_{m3} are present in its expression. This can be seen by substituting the value of g_{m1} and g_{m3} in Eq. 4.1 to give

$$L_{eq} = \frac{4V_T{}^2 C_2}{I_{B1} I_{B3}}$$

4.3.1 Experimental Results

In order to investigate the operation of this inductor, the circuit shown in Fig. 4.2 was used. C_2, C_x were chosen as 0.01μF, I_{B3} was fixed at 38μA and R_s as 470KΩ. With these values, L_{eq} was calculated as

$$L_{eq}(calculated) = \frac{0.597}{I_{B1}}\text{H}$$

(where the "micro" part of I_{B1} (10^{-6}) has already been taken into account in the above expression) and measured value as

$$L_{eq}(measured) = \frac{2.533}{f_r{}^2}\text{H}$$

(where the "mega" part of $f_r{}^2$ (10^6)has already been taken into account in the above expression).

Table 4.2 shows the measured and calculated results, along with the percentage error between the two. Fig. 4.5 shows the same information plotted as a graph. It is obvious from the Table that there is big discrepancy between the measured and calculated readings due to the presence of two g_m terms in the expression of L_{eq}.

It should be pointed out here that range of inductance obtained form this circuit could be much more than what is depicted in the Table. In other words, unlike the previous circuit, where, due to the circuit instability, the value of I_{B1} could go upto a maximum value of around 55μA, the I_{B1} values and the corresponding L_{eq} values, in this case, were not restricted to what is shown. A fewer readings were taken, in order to compare the results of various circuits for almost the same range of I_B values. As a matter of fact, the circuit has the advantage of generating a large range of inductance values.

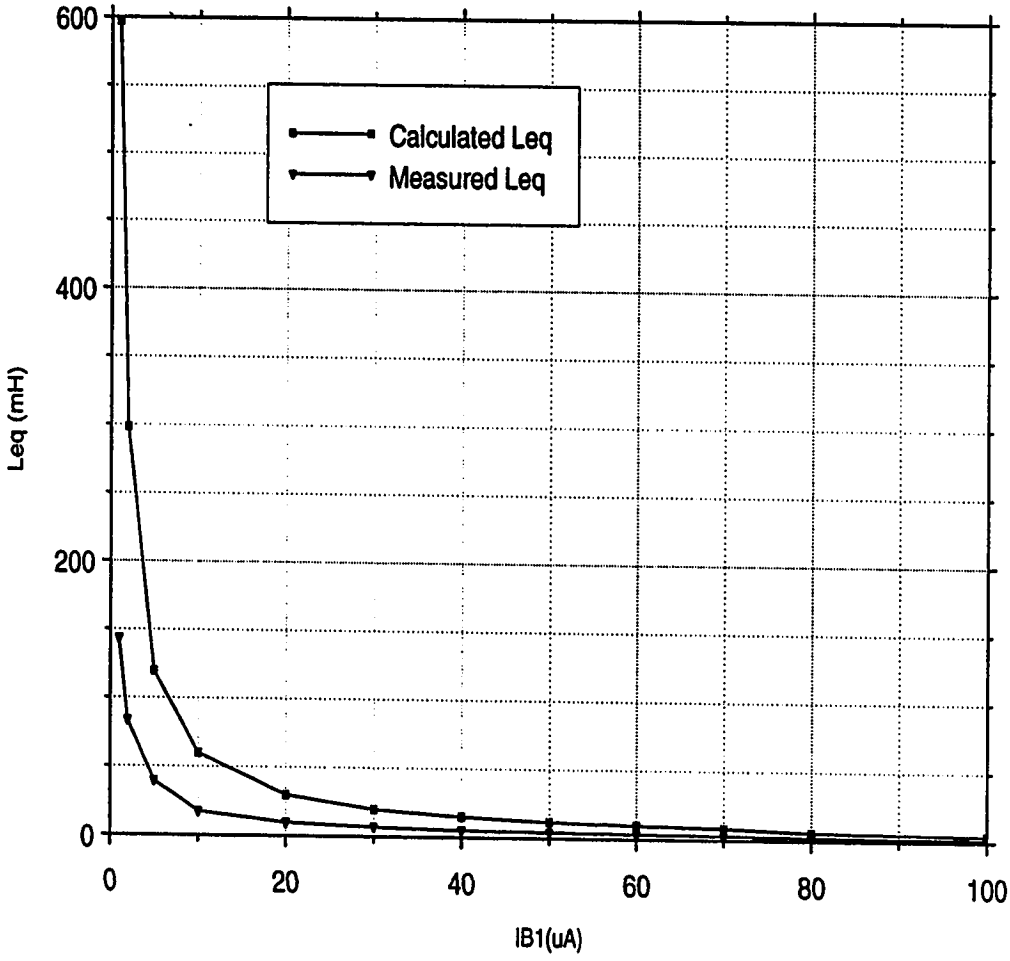

Figure 4.5: Graph between L_{eq} and I_{B1} for the OTA based temperature-dependent inductor.

I_{B1} (μA)	L_{eq}(measured) (mH)	L_{eq}(calculated) (mH)	% error (%)
1	143.6	597	75.95
2	83.74	298.5	71.95
5	39.58	119.4	66.85
10	17.60	59.7	70.52
20	9.9	29.85	66.83
30	7.02	19.9	64.7
40	5.23	14.92	64.95
50	4.4	11.94	63.15
60	3.75	9.95	62.31
70	3.23	8.53	62.13
80	2.47	5.97	58.63
100	1.85	4.26	56.57

Table 4.2: Comparison of measured and calculated values of L_{eq} for the OTA based temperature-dependent inductor.

4.4 OTA and Op-amp Based Temperature-Independent Inductor

In an attempt to overcome the problem of temperature-dependency faced in the previous section a GIC circuit, shown in Fig. 2.5, was designed and developed. The circuit's input impedance is a parallel combination of impedances, Z_7 and $(Z_5Z_7)/(g_{m1}g_{m3}Z_2Z_4Z_6)$ respectively. The latter is of actual use and importance, since it can simulate different circuit elements. In order to minimize the effect of the presence of Z_7, it is recommended to connect a resistor, R_7 of a large value in place of Z_7.

This circuit can simulate a temperature-insensitive inductor if we make the the

following replacements in the original circuit: $Z_2 = \frac{1}{g_{m2}}$, $Z_4 = \frac{1}{g_{m4}}$, $Z_5 = R_5$, $Z_7 = R_7$ and $Z_6 = \frac{1}{C_6 s}$. The resulting value of the inductor will be

$$L_{eq} = \frac{I_{B2} I_{B4} R_5 R_7 C_6 s}{I_{B1} I_{B3}}$$

Thus using this scheme, a temperature-independent[2], voltage/current controlled grounded inductor can be realized.

4.4.1 Experimental Results

The operation of the simulated inductor was tested using the tuned circuit of Fig. 4.2. The values of the components and currents chosen for the experiment were as follows.

$C_6 = C_x = 0.01\mu$F, $R_5 = 1$KΩ, $R_7 = 500$KΩ, $I_{B1} = I_{B2} = 61.1\mu$A, $I_{B4} = 6.4\mu$A and $R_s = 1$MΩ. CA741 type op-amps were used. With these values, L_{eq} was calculated as

$$L_{eq}(calculated) = \frac{3.2}{I_{B3}}\text{H}$$

(where the "micro" part of I_{B1} (10^{-6}) has already been taken into account in the above expression) and measured value as

$$L_{eq}(measured) = \frac{2.533}{{f_r}^2}\text{H}$$

(where the "mega" part of ${f_r}^2$ (10^6)has already been taken into account in the above expression).

[2]Independent of V_T

Measured and calculated values are given in Table 4.3 and plotted in Fig. 4.6. The range of the simulated inductance is set by the instability of the circuit. It was found out that for I_{B3} around 50μA, the circuit produced oscillations.

Comparing the results of this section with those of the preceding one, it can be observed that, since the expression of the simulated inductance, L_{eq}, is independent of g_m terms, the theoretical and experimental readings are in better agreement.

I_{B3} (μA)	L_{eq}(measured) (mH)	L_{eq}(calculated) (mH)	% error (%)
1	2093	3200	34.6
3	990	1070	7.48
5	782	640	22.19
10	405	320	26.56
15	264	213	23.94
20	175	160	9.4
25	144	128	12.5
30	105	107	1.9
35	80	91	12
40	70	80	12.5
45	55	71.1	22.64
50	47.5	64	25.8

Table 4.3: Comparison of measured and calculated values of L_{eq} for the OTA and op-amp based temperature-independent inductor.

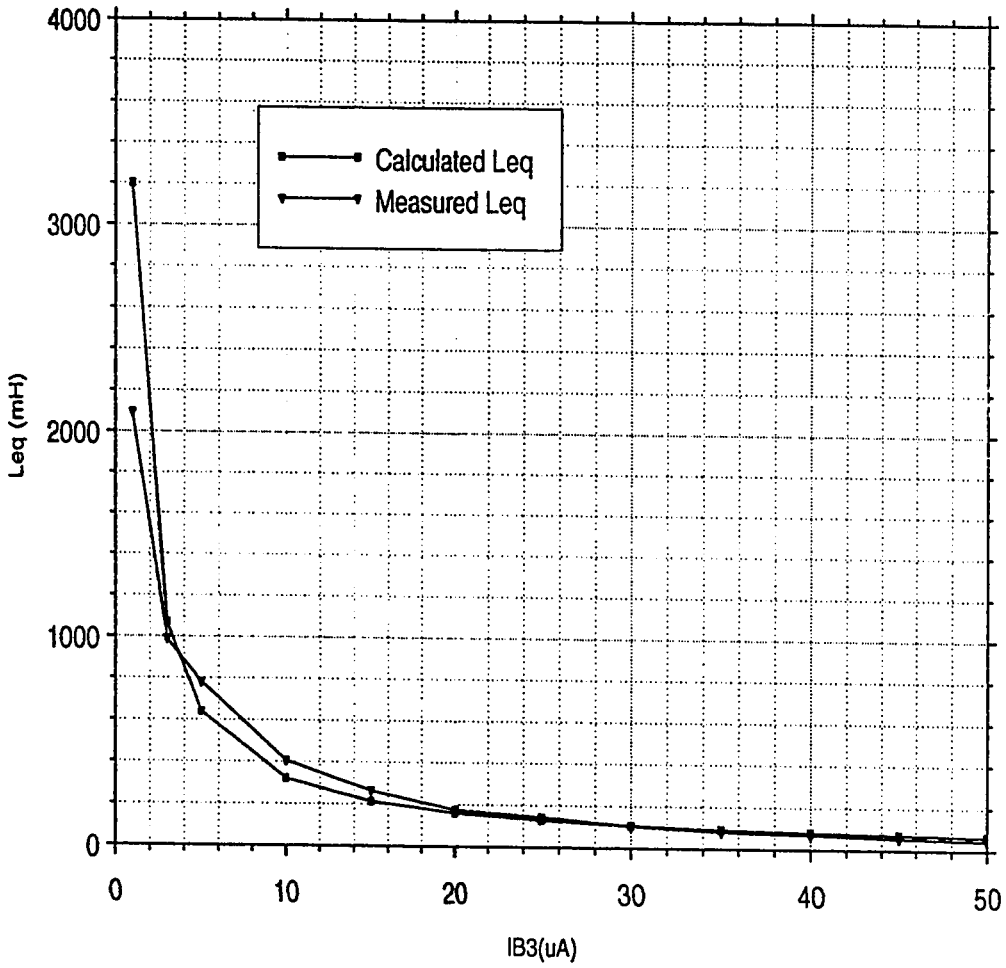

Figure 4.6: Graph between L_{eq} and I_{B3} for the OTA and op-amp based temperature-independent inductor.

4.5 A CCII+ Based Temperature-Dependent Inductor

In Chapter 2, it was shown how CCIIs could be used to simulate various circuit elements when connected in general impedance convertor (GIC) circuits. One such circuit was shown in Fig. 2.6. A voltage/current controlled, grounded inductor can be realized using this circuit, if we make the following substitution in the said circuit: $Z_1 = -\frac{1}{g_{m1}}$, $Z_3 = R_3$ and $Z_2 = \frac{1}{C_2 s}$.

Now the input impedance, Z_{in}, can be expressed as

$$Z_{in} = \frac{R_3 C_2 s}{g_{m1}}$$

which is equivalent to an inductor, L_{eq} given by

$$L_{eq} = \frac{R_3 C_2}{g_{m1}}$$

Thus, an ideal, grounded, voltage/controlled inductor is realized which is tunable with the biasing current or voltage.

4.5.1 Experimental Results

Experimental verification of the circuit's performance was obtained using the tuned circuit shown in Fig. 4.2. Using $R_3 = 10\text{K}\Omega$, $R_s = 470\text{K}\Omega$ and $C_2 = C_x = 0.01\mu\text{F}$, the value of the inductance is calculated as

$$L_{eq}(calculated) = \frac{4.762}{I_{B1}}\text{H}$$

(where the "micro" part of I_{B1} (10^{-6}) has already been taken into account in the above expression) and the measured value is computed using

$$L_{eq}(measured) = \frac{2.533}{f_r^{\,2}}\text{H}$$

(where the "mega" part of $f_r^{\,2}$ (10^{6})has already been taken into account in the above expression)

Table 4.4 shows the experimental and theoretical results. It also gives the discrepency between the two readings as percentage error. In Fig. 4.7 these results are plotted as a function of I_{B1}. It is obvious from these results that due to the presence of g_{m1} term in the expression of L_{eq}, the measured and calculated results are not in close agreement. Moreover, the circuit instabilities restrict the range of inductance values to that shown in the Table.

In order to eliminate the temperature-dependency of the circuit, another all CCII based circuit shown in Fig. 2.7 is used in the next section.

4.6 A CCII+ Based Temperature-Independent Inductor

Refer to Fig. 2.7 in Chapter 2. A positive inductance can be obtained from this structure by having, $Z_1 = -\frac{1}{g_{m1}}$, $Z_2 = \frac{1}{g_{m2}}$, $Z_3 = R_3$, $Z_4 = \frac{1}{C_4 s}$, $Z_5 = R_5$ and thus

$$L_{eq} = \frac{g_{m2} R_3 R_5 C_4}{g_{m1}}$$

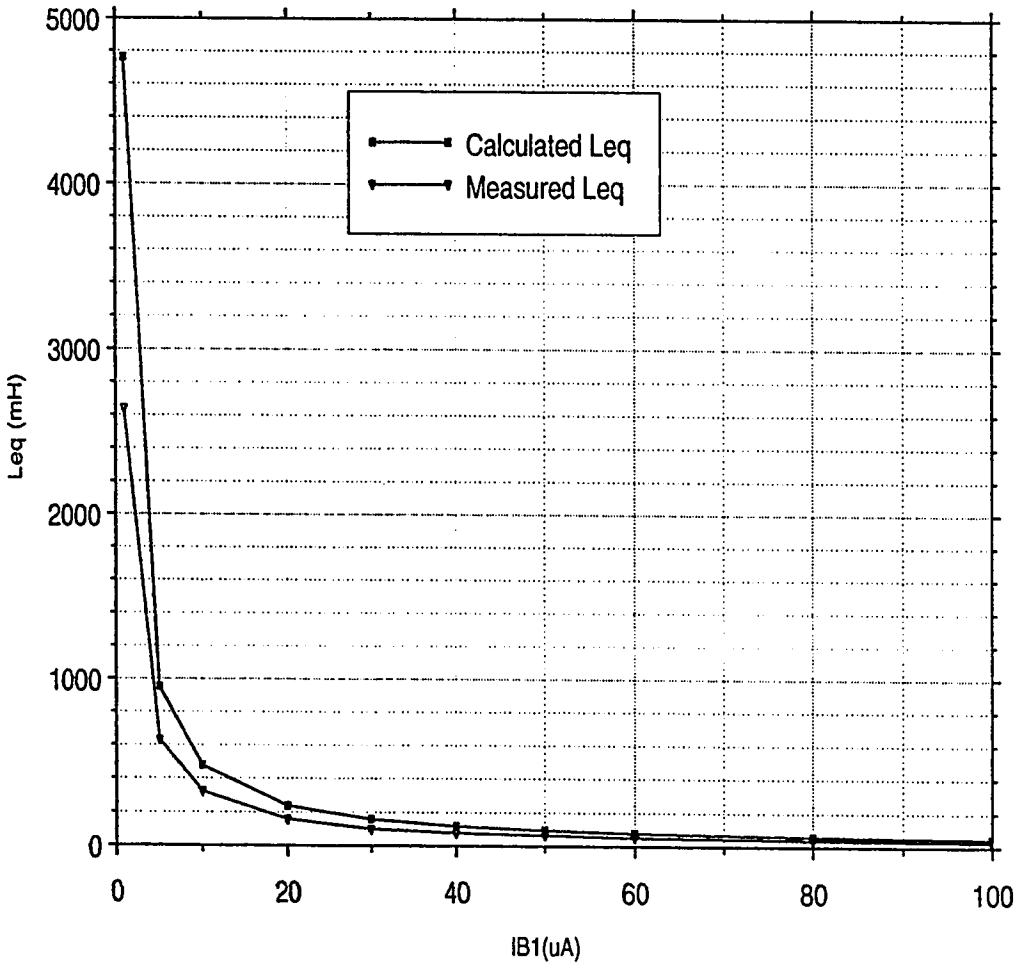

Figure 4.7: Graph between L_{eq} and I_{B1} for the CCII based temperature-dependent inductor.

I_{B1} (μA)	L_{eq}(measured) (mH)	L_{eq}(calculated) (mH)	% error (%)
1	2640	4762	44.50
5	633.25	952.4	33.50
10	323.10	476.2	32.15
20	158.31	238.1	33.50
30	101.32	158.73	36.20
40	77.96	119.05	34.50
50	65.9	95.24	30.80
60	51.70	79.36	34.80
80	39.58	59.52	33.50
100	31.27	47.62	34.33

Table 4.4: Comparison of measured and calculated values of L_{eq} for the CCII based temperature-dependent inductor.

For practical realisation of this circuit, following component values and currents were used: $R_3 = R_4 = 200\Omega$, $C_4 = 0.1\mu$F and I_{B2} was fixed at 129.5μA. This gives inductance value of

$$L_{eq} = \frac{0.518}{I_{B1}}\text{H}$$

(where the "micro" part of I_{B1} (10^{-6}) has already been taken into account in the above expression).

4.6.1 Experimental Results

To verify the theory by measurements, the simulated inductor was connected in a sinusoidal oscillator configuration as shown in Fig. 4.8. A simple analysis shows

that for this circuit, frequency of oscillation, f_o is given by

$$f_o = \frac{1}{2\pi\sqrt{L_{eq}C_x}}$$

and the condition of oscillation is given by

$$1 = g_m R$$

The negative resistor $-\frac{1}{g_m}$ in this configuration is obtained by using the circuit of Fig. 3.2 shown in Chapter 3. Following values of components and currents were used: $R = 10\text{K}\Omega$, $C_x = 0.1\mu\text{F}$, $I_B = 12.3\mu\text{A}$. With these values, the frequency of oscillation, f_o is calculated as

$$f_o(calculated) \approx 0.7\sqrt{I_{B1}}\text{KHz}$$

Measured and calculated results for f_o are shown in Table 4.5 as a function of current I_{B1}. The Table also shows the discrepency between the two readings. This data is also plotted in Fig. 4.9. It was observed that for values of I_{B1} less than 10μA and around 85μA the signal became distorted and disappeared altogether around 90μA. Good quality sine waves had been obtained over the entire tuning range controlled by I_{B1}. However, it is suggested to operate the circuit for I_{B1} values upto 50μA, since beyond that, the circuit shows larger discrepency between measured and calculated data.

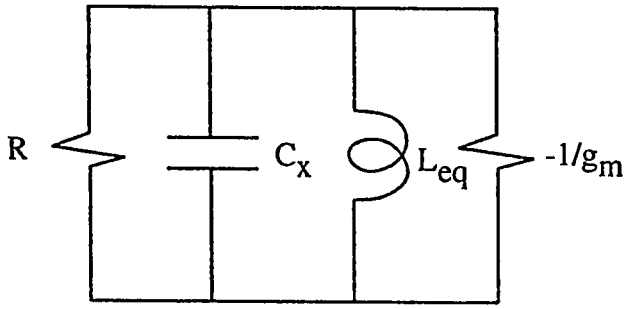

Figure 4.8: Oscillator circuit to verify the operation of simulated inductor.

I_{B1} (μA)	f_o(measured) (KHz)	f_o(calculated) (KHz)	% error (%)
10	2.0	2.20	9.10
15	2.63	2.71	2.95
20	3.12	3.13	0.32
25	3.57	3.50	2.00
30	4.0	3.83	4.44
35	4.44	4.14	7.25
40	5.0	4.43	12.87
50	5.88	4.95	18.80
60	6.85	5.40	26.85
70	7.81	5.86	33.30
80	8.93	6.26	42.65
85	10.0	6.45	55.00

Table 4.5: Comparison of measured and calculated values of f_o for the CCII based temperature-independent inductor.

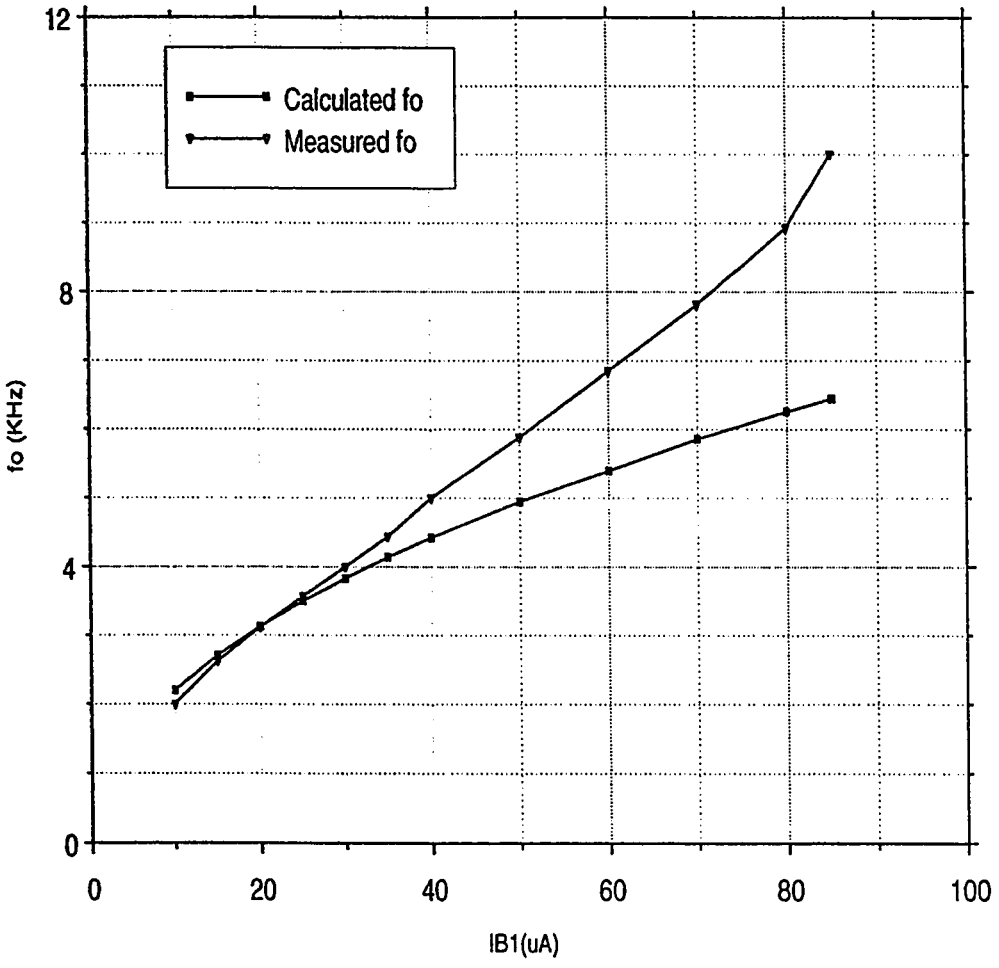

Figure 4.9: Graph between f_o and I_{B1} for the CCII based temperature-independent inductor.

4.7 Single Op-amp Based Grounded Inductor

All the simulated inductor circuits described so far require at least two active elements. In this section, we will present a circuit which employs only one op-amp, as active device, to obtain a grounded voltage/current controlled inductor. In other words, the circuit enjoys the attractive feature of low component count over the others discussed thus far. This inductor is realisable by having, $Z_1 = -\frac{1}{g_{m1}}$, $Z_2 = \frac{1}{C_2 s}$ and $Z_3 = R_3$ in the circuit shown in Fig. 2.4 in Chapter 2. With this selection the equivalent inductance, L_{eq}, is given by

$$L_{eq} = \frac{R_3 C_2}{g_{m1}}$$

which is an ideal grounded, voltage/current controlled inductor.

4.7.1 Experimental Results

The operation of the said inductor is practically verified by using the oscillator circuit of Fig. 4.8. Following selections were made: $C_2 = C_x = 0.01\mu$F, $R = 10$KΩ, $R_3 = 1$KΩ and $I_B = 5\mu$A. With these values, the frequency of oscillation, f_o was calculated as

$$f_o(calculated) \approx 2.25\sqrt{I_{B1}}\text{KHz}$$

Table 4.6 shows the theoretical and experimental values of f_o as a function of current I_{B1}. It also gives the error between the two readings. Fig. 4.10 shows the graph of these results. It was found out that for values of I_{B1} less than 5μA the

signal became distorted and died out for I_{B1} greater than 450μA. A good quality sine wave was obtained over the entire tuning range controlled by I_{B1}. However, for higher I_{B1} values (around 300μA) the discrepency between measured and calculated results increased.

I_{B1} (μA)	f_o(measured) (KHz)	f_o(calculated) (KHz)	% error (%)
5	5.5	5.0	11.00
10	7.57	7.11	6.47
20	10.42	10.0	4.2
30	12.5	12.32	1.46
40	13.89	14.23	2.39
50	15.4	15.9	3.14
60	16.67	17.43	4.36
70	17.54	18.82	6.80
60	18.51	20.0	7.45
90	19.23	21.34	9.88
100	20.41	22.51	9.3
120	21.74	24.65	11.8
150	23.8	27.56	13.64
200	26.3	31.82	17.35
250	29.4	35.57	17.35
300	31.25	38.97	19.81
400	35.1	45.0	22.00
450	35.7	47.73	25.20

Table 4.6: Comparison of measured and calculated values of f_o for the single op-amp based inductor.

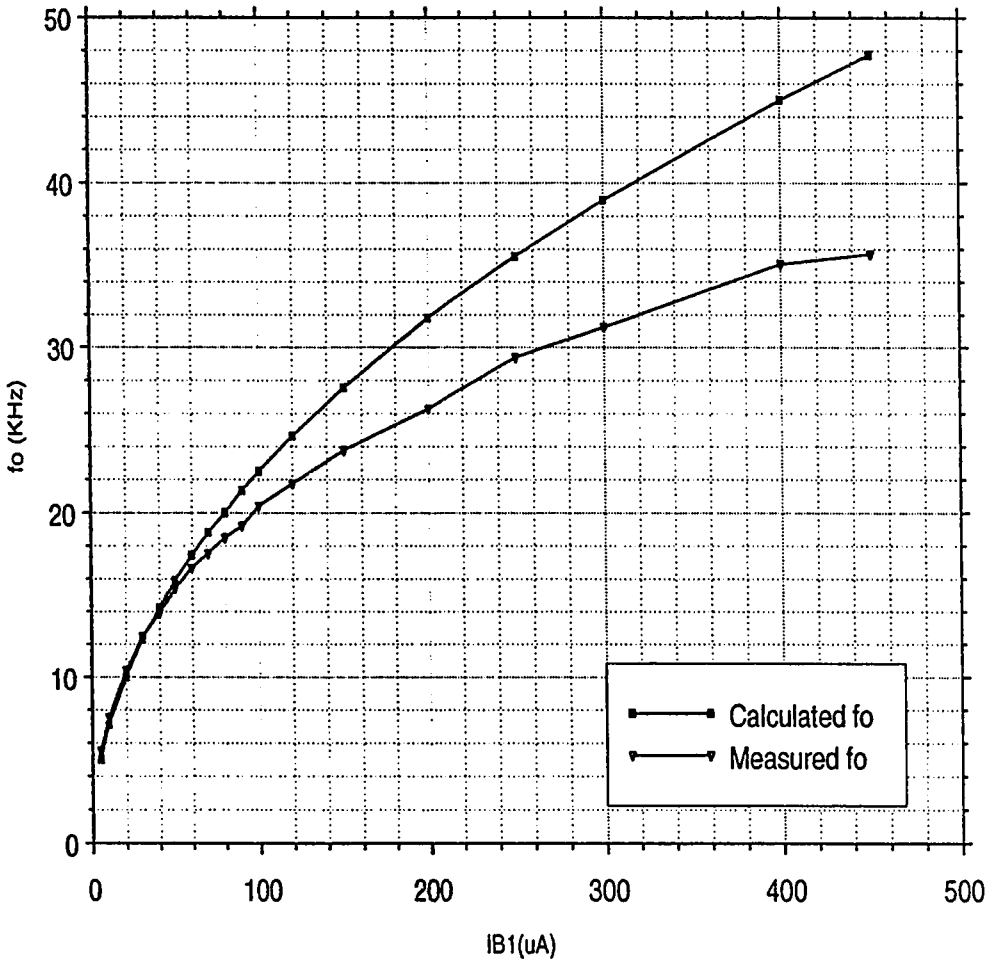

Figure 4.10: Graph between f_o and I_{B1} for the single op-amp based inductor.

Chapter 5

Stability of Simulated Circuits

5.1 Introduction

It was shown in the last two chapters, how voltage/current controlled (digitally programmable) inductor and capacitor circuits could be simulated using passive components and active elements. It could be noticed that all these circuits required at least one active element, in addition to one or more passive components. In addition, all the circuits were analysed assuming the active devices as ideal. However, we know that, in reality, these devices do deviate from ideal behaviour. These non-idealities could result from the finite input/output impedance, finite gain, frequency dependence of the gain, limited dynamic range and so on. The non-idealities do affect the operation and performance of these simulated elements to some extent. As a matter of fact, they set a limit on the range of simulated values obtainable

from these circuits.

In other words, all these circuits, composed of many capacitors, (some external and many other inside each active device), may exhibit instability in the form of oscillations, when certain conditions are met by changing some circuit parameters (the biasing voltage/current of the OTA). This raises the need to investigate the stability of these circuits and is therefore the objective of this chapter.

There could be two approaches to study the instability of a simulator circuit. In the first approach, non-idealities of the active element(s) are taken into consideration and the input impedance of the circuit is derived again. This results in a very tedious procedure of transforming complex mathematical expressions into their corresponding impedance models. In the second approach, characteristic equation of the circuit is obtained, including the non-idealities of the circuit, to check whether the circuit oscillates or not. This technique is relatively simpler. We shall use both techniques in this chapter.

We start with the first approach and present subsequently, the effect of the non-ideal behaviour of active elements on the input impedance of a simulator circuit.

5.2 Effect of Non-idealities on the Input Impedance of an Inductor Simulator Circuit

Consider, for example, the inductor simulator circuit of Fig. 4.1 discussed in Chapter 4 and redrawn in Fig. 5.1. For simplicity we assume $R_3 = R_4 = R$ and $C_5 = C$.

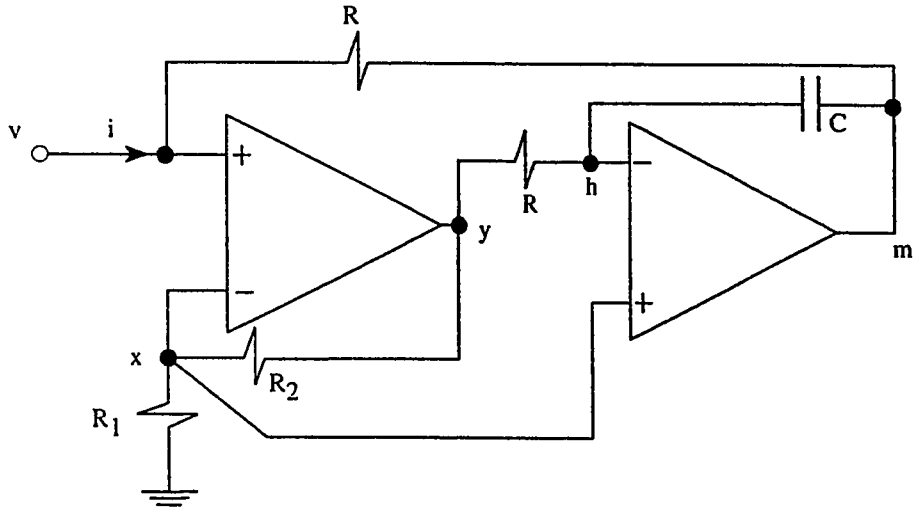

Figure 5.1: The inductor simulator circuit analysed for the input imedance.

Analysing the circuit, we have,

$$x = (\frac{R_1}{R_1 + R_2})y$$

or

$$x = \alpha y \tag{5.1}$$

where

$$\alpha = \frac{R_1}{R_1 + R_2}$$

Also

$$y = (v - x)G \tag{5.2}$$

Substituting Equation 5.1 in 5.2, we get,

$$y = (\frac{G}{1 + \alpha G})v \tag{5.3}$$

Now

$$m = (x - h)G$$

or

$$m = G(\alpha y - h) = G(\frac{\alpha G v}{1 + \alpha G} - h) \tag{5.4}$$

At node h,

$$h = (\frac{1}{1 + RCs})y + (\frac{RCs}{1 + RCs})m \tag{5.5}$$

Putting y from Equation 5.3 in Equation 5.5 gives

$$h = (\frac{G}{(1 + RCs)(1 + \alpha G)})v + (\frac{RCs}{1 + RCs})m$$

Substituting this value in Equation 5.4, we get

$$m = \frac{(\alpha G^2(1 + RCs) - G^2)v}{(1 + \alpha G)(1 + RCs(1 + G))} \tag{5.6}$$

Now the current, i, is given by

$$i = \frac{v - m}{R}$$

Substituting Equation 5.6 in above Equation we get,

$$i = [\frac{1}{R} - \frac{\alpha G^2(1 + RCs) - G^2}{R(1 + \alpha G)(1 + RCs(1 + G))}]v$$

or

$$\frac{i}{v} = \frac{1}{R} + \frac{G^2 - \alpha G^2}{R(1+\alpha G)(1+RCs(1+G))} - \frac{RCG^2\alpha s}{R(1+\alpha G)(1+RCs(1+G))} \qquad (5.7)$$

Now consider the second term on right hand side of Equation 5.7, which can be written as

$$\frac{1}{[R(1+\alpha G)]/[G^2(1-\alpha)] + [R^2(1+G)(1+\alpha G)Cs]/[G^2(1-\alpha)]}$$

and is equivalent to a resistor,

$$\frac{R(1+\alpha G)}{G^2(1-\alpha)}$$

in series with an inductor,

$$\frac{R^2(1+G)(1+\alpha G)C}{G^2(1-\alpha)}.$$

Now consider the third term on right hand side of Equation 5.7, which can be written as

$$-\frac{1}{[(1+\alpha G)s]/[CG^2\alpha] + [R(1+\alpha G)(1+G)]/[\alpha G^2]}$$

and hence is equivalent to a negative resistor,

$$-\frac{R(1+\alpha G)(1+G)}{\alpha G^2}$$

in series with a negative capacitor,

$$-\frac{G^2\alpha C}{(1+\alpha G)}.$$

Consequently, the input impedance, Z_{in} $(\frac{v}{i})$, of this simulator circuit is represented by the circuit shown in Fig. 5.2. It can be easily seen from this figure that the

input impedance is no longer a simple lossless grounded inductor as the ideal analysis predicts. Rather it involves, now, a negative resistor and a negative capacitor, in addition to other elements. Hence as such the circuit is prone to oscillations.

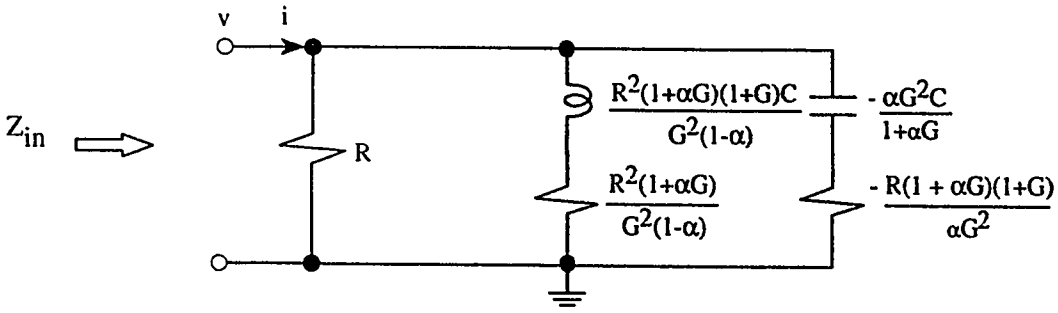

Figure 5.2: The resulting input impedance of the inductor simulator circuit.

It is clear from the above discussion, that a very involved analysis results even when we consider only one non-ideality in the circuit, viz. the finite gain of the op-amps, and try to study the instability of the simulator circuits. Moreover, the resulting circuit does not give a direct insight about the circuit's instability. Therefore, subsequently, we will analyse this circuit using the second approach, that is, by obtaining its characteristic equation, which is a relatively simpler and straightforward technique.

5.3 Instability Study of the Inductor Simulator Circuit

Refer to the circuit shown in Fig. 4.1, which has been redrawn in Fig. 5.3.

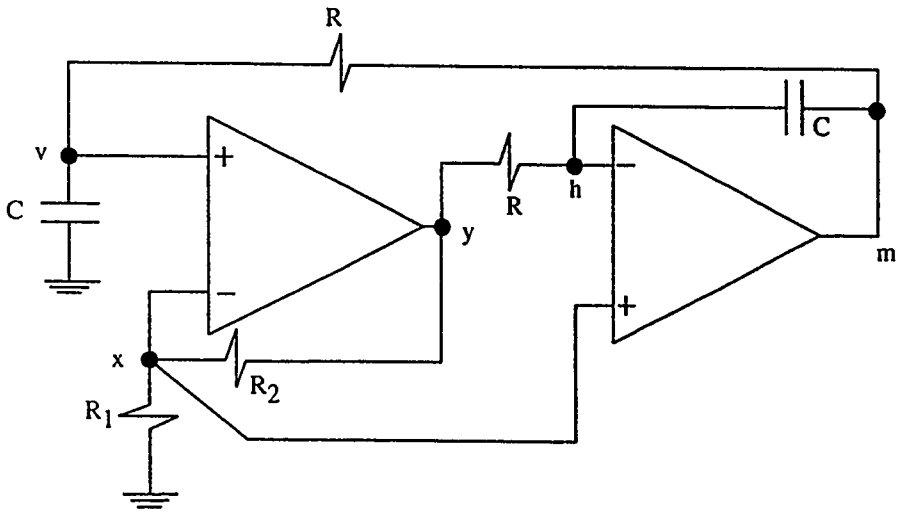

Figure 5.3: The inductor simulator circuit considered for stability study.

The operation of this inductor was verified by connecting it in the parallel tuned circuit of Fig. 4.2. Therefore, we should also take into consideration the effect of R_s and C_x on the stability of the circuit. However, since R_s used was relatively large (1MΩ), we shall ignore it to simplify the analysis. Moreover, let $C_x = C_5 = C$ and assume that the two op-amps are identical and have infinite input resistances and zero output resistances. The only non-ideality considered will be the finite frequency-dependent gain of the op-amps, i.e. the open loop gain of the op-amps

will be modelled by

$$G_i(s)\,|_{(i=1,2)} = \frac{B}{s} \tag{5.8}$$

where B is the gain bandwidth product of the op-amps. A simple analysis gives

$$m = G(s)(x - h) \tag{5.9}$$

$$y = G(s)(v - x) \tag{5.10}$$

$$x = \frac{R_1 y}{R_1 + R_2} \tag{5.11}$$

$$m = \frac{(R + Z)v}{Z} \tag{5.12}$$

$$\frac{(R + Z)h}{RZ} = \frac{y}{R} + \frac{m}{Z} \tag{5.13}$$

where $Z = \frac{1}{Cs}$.

Using Equations 5.9 to 5.13, the characteristic equation of the circuit can be expressed as:

$$(1 + RCs)B^2\alpha = B^2 + (1 + RCs)(s + \alpha B)RCBs + (1 + RCs)^2(s + \alpha B)s \tag{5.14}$$

where

$$\alpha = \frac{R_1}{R_1 + R_2}$$

Now by comparing the real and imaginary parts on both sides of Equation 5.14, i.e. using the Barkhausen criterion, the frequency of oscillation of the simulator

circuit is given by

$$\omega_o{}^2 = \frac{\alpha B}{R^2C^2B(1+\alpha)+2RC} \tag{5.15}$$

and the condition of oscillation can be expressed as

$$R^2C^2\left(\frac{\alpha B}{R^2C^2B(1+\alpha)+2RC}\right)^2 + (1-\alpha)B^2 = (1+RCB(1+2\alpha)+R^2C^2B^2\alpha)\left(\frac{\alpha B}{R^2C^2B(1+\alpha)+2RC}\right) \tag{5.16}$$

It is clear from the above analysis that if Equation 5.16 is satisfied, the circuit may run into oscillation. In other words, the circuit may show instability for practical values of active and passive parameters.

Similar analysis could be carried out in order to verify the stability of any simulator circuit.

5.4 Instabilities in Carlosena's Circuits

Carlosena et al. have reported in [23] a number of resistively variable capacitor (RVC) circuits. Out of these, three have been proposed as optimum (i.e. their performance appeared sufficiently good in terms of bandwidth and highest achievable capacitance value). In an attempt to introduce digital programmability into these circuits, they were practically implemented. However, it was noticed that all the three circuits exhibited instability when oscilloscope probe was connected at their inputs. In other words, the circuits were oscillatory under certain conditions.

In the following, we will apply the characteristic equation approach to show the instability of one of these three circuits. By the same notion, other two circuits could also be proved to be unstable.

Refer to Fig. 5.4, which is shown as Fig. 8(iG) in [23], except with the addition of C_p and R_p which represent the oscilloscope probe and input capacitance and resistance repectively [26].

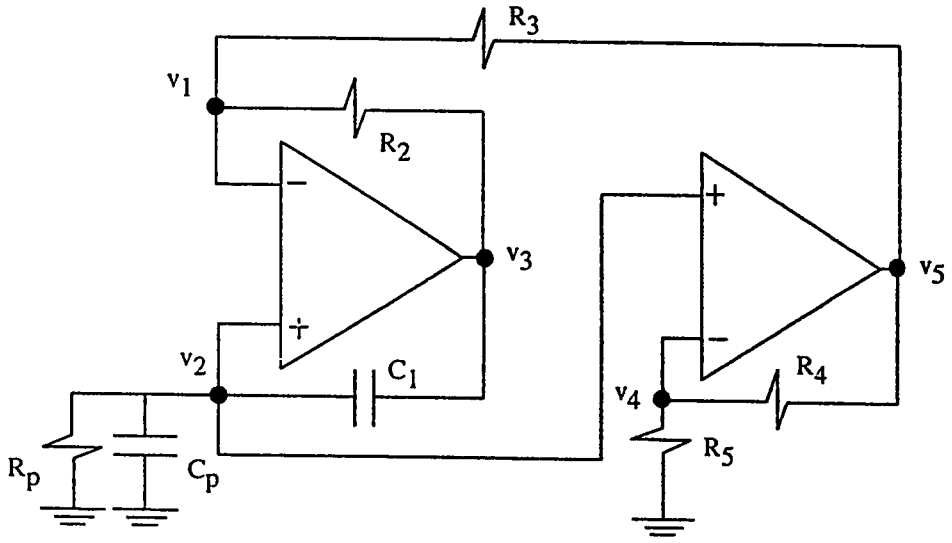

Figure 5.4: The unstable circuit reported in [23].

Like the previous section, to simplify analysis, we shall assume the two op-amps identical and use the single pole model of Equation 5.8 for the open-loop gain, $G(s)$, of the op-amp as the only non-ideality.

A simple analysis gives

$$v_3 = (v_2 - v_1)G(s) \tag{5.17}$$

$$v_5 = (v_2 - v_4)G(s) \tag{5.18}$$

$$v_4 = \alpha v_5 \tag{5.19}$$

where

$$\alpha = \frac{R_5}{R_4 + R_5}$$

Equations 5.18 and 5.19 gives

$$v_5 = \frac{G(s)v_2}{1 + \alpha G(s)} \tag{5.20}$$

Also

$$v_3 = (\frac{Z_1 + Z_p}{Z_p})v_2 \tag{5.21}$$

where

$$Z_p = \frac{R_p}{1 + R_p C_p s}$$

and

$$v_1\beta = \frac{v_3}{R_2} + \frac{v_5}{R_3} \tag{5.22}$$

where

$$\beta = \frac{R_2 + R_3}{R_2 R_3}$$

Substituting Equation 5.21 in Equation 5.17 yields

$$v_1 = (\frac{G(s)Z_p - Z_1 - Z_p}{G(s)Z_p})v_2 \tag{5.23}$$

Substituting Equations 5.20 and 5.21 in Equation 5.22, we get,

$$v_1\beta = (\frac{Z_1 + Z_p}{R_2 Z_p})v_2 + (\frac{G(s)}{(1 + \alpha G(s))R_3})v_2 \tag{5.24}$$

Substituting v_1 from Equation 5.23 in Equation 5.24 gives

$$\beta(\frac{G(s)Z_p - Z_1 - Z_p}{G(s)Z_p}) = \frac{Z_1 + Z_p}{R_2 Z_p} + \frac{G(s)}{(1 + \alpha G(s))R_3} \tag{5.25}$$

Further simplification yields

$$Z_p R_3(G(s) + R_2\beta) + Z_P R_3 \alpha G(s)(G(s) + R_2\beta) + Z_1 R_3(G(s) + R_2\beta) +$$

$$Z_1 R_3 \alpha G(s)(G(s) + R_2\beta) + Z_p R_2 G(s)^2 = Z_p R_2 R_3 \beta G(s)(1 + \alpha G(s)) \tag{5.26}$$

Now substituting

$$Z_p = \frac{R_p}{1 + R_p C_p}$$

$$G(s) = \frac{B}{s}$$

and

$$Z_1 = \frac{1}{C_1 s}$$

in Equation 5.26 and simplifying we get the characteristic equation of the circuit as,

$$R_p R_3 C_1(B + R_2\beta s)s^2 + R_P R_3 C_1 B\alpha(B + R_2\beta s)s +$$

$$R_3(1 + R_p C_p s)(B + R_2\beta s)s + R_3 B\alpha(1 + R_p C_p s)(B + R_2\beta s) +$$

$$R_p R_2 C_1 B^2 s = R_p R_2 R_3 C_1 B\beta(s + B\alpha)s \tag{5.27}$$

Now, comparison of real quantities on both sides of Equation 5.27 and simplification gives

$$[R_p C_1 B + R_P R_2 C_1 B\alpha\beta + R_2\beta + R_p R_2 C_p B\alpha\beta - R_p R_2 C_1 B\beta]\omega^2 = B^2\alpha \tag{5.28}$$

Similarly, comparing imaginary quantities on both sides of Equation 5.27 and simplifying, we get,

$$[R_pR_2R_3C_1\beta + R_PR_2R_3C_p\beta]\omega^2 = R_pR_3C_1B^2\alpha + R_3B + R_pR_3C_pB^2\alpha + R_2R_3B\alpha\beta + R_pR_2C_1B^2 - R_pR_2R_3C_1B^2\alpha\beta \quad (5.29)$$

From the last two equations we can obtain the frequency of oscillation as

$$\omega_o{}^2 = \frac{R_pR_3B^2\alpha(C_1 + C_p) + R_3B(1 + R_2\alpha\beta) + R_pR_2C_1B^2(1 - R_3\alpha\beta)}{R_pR_2R_3\beta(C_1 + C_p)} \quad (5.30)$$

and the condition of oscillation as

$$R_pR_2R_3B^2\beta\alpha(C_1 + C_p) = [R_pR_3B^2\alpha(C_1 + C_p) + R_3B(1 + R_2\alpha\beta) + R_pR_2C_1B^2(1 - R_3\alpha\beta)][R_pC_1B(1 + R_2\alpha\beta) + R_2\beta + R_pR_2B\beta(C_p\alpha - C_1)] \quad (5.31)$$

It can be seen from Equations 5.30 and 5.31 that there is a possibility that the circuit may oscillate when certain conditions, depending on the practical values of active and passive parameters, are met.

To prove this point further, the said circuit was verified experimentally. The same values of the components were used as reported in [23], except that a $10nF$ capacitor was used instead of $8nF$ as C_5. uA741 type op-amps were used with dc supply voltage of $\pm$15V. Experimental results proved the circuit to be oscillatory and Fig. 5.5 shows these osillations. The frequency of oscillation was measured as 6.6KHz, while V_P(+ive) = 14V and V_P(-ive) = 13V.

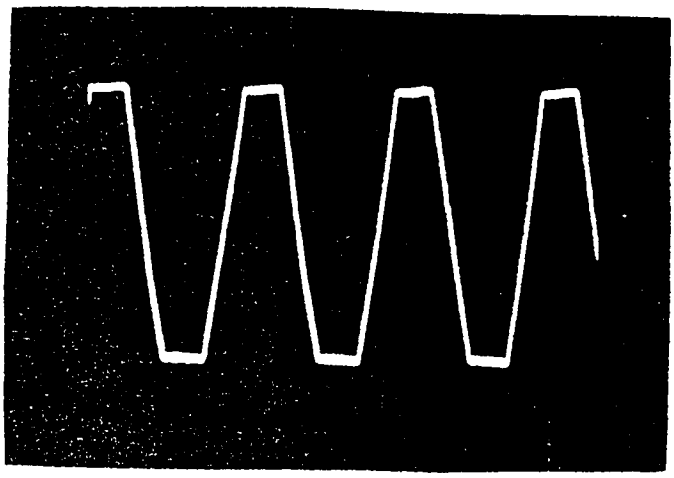

Figure 5.5: Experimental results for the unstable circuit reported in [23], V_P(+ive) = 14V, V_P(-ive) = 13V and f_o = 6.6KHz.

SPICE simulation was also carried out using the uA741 op-amp model available in the built-in library of SPICE called EVAL.LIB. A dc supply voltage of ±15V was used. To initiate oscillations, a noise voltage was simulated by the following SPICE command.

V_{NOISE} N1 N2 PWL(0 50V 10N 50V 10.001N 0V)

where N1 and N2 are the nodes across which this noise voltage source is connected.

The simulation results are shown in Fig. 5.6. The frequency of oscillation can easily be obtained from this plot as 5.5KHz, which is in good agreement with the measurements.

Following the same procedure, the other two circuits were also found out to

exhibit instability. Thus it can be concluded that these realizations for the resistively variable capacitors have the tendency to produce oscillations under certain conditions.

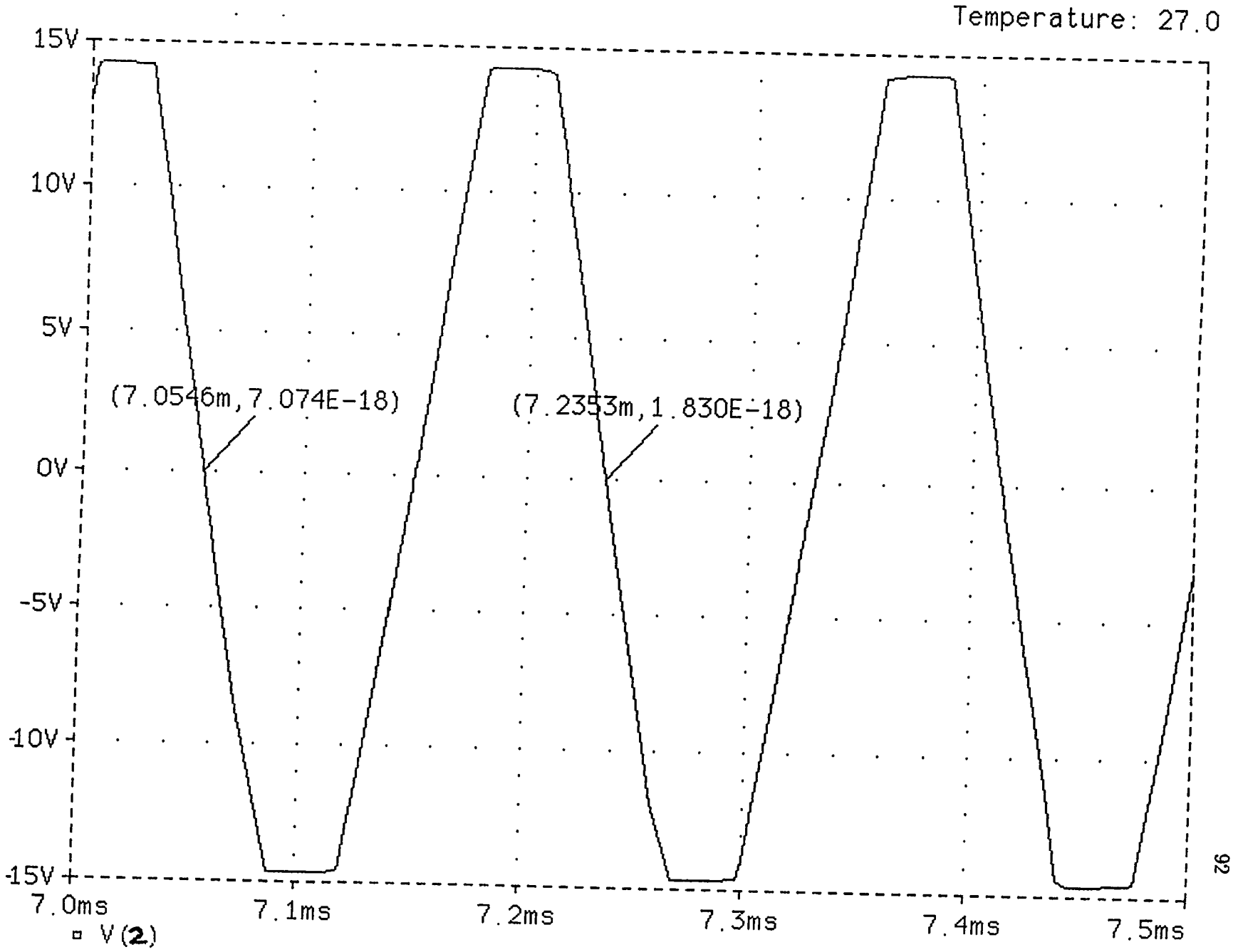

Figure 5.6: SPICE simulation results for the unstable circuit reported in [23].

Chapter 6

Conclusion and Future Work

6.1 Introduction

In this thesis, we have presented a number of Digitally Programmable Temperature-Independent Tuned (DiPTIT) circuits. These circuits simulate variable (volatge/current controlled) capacitors and inductors. In this chapter, we will draw some conclusions regarding this work. We will then discuss some important extensions that can be undertaken if somebody intends to work further in this area.

6.2 Conclusions

The programmable feature of operational transconductance amplifier (OTA) has been exploited in this work to realize digitally programmable circuit elements. The

inherent temperature-dependence of OTA's gain, g_m, has been countered to accomplish temerature-independence[1] in the circuit while retaining its voltage/current control feature. These features were incorporated in some of the existing circuits while some new circuits were designed with these features, during the course of this work.

Op-amps, OTAs and second generation current conveyors (CCII+), three widely used active elements, were used in this work. Of these, OTA and CCII based circuits could work at high frequencies, too.

The simulator circuits were practically implemented to verify the theory. Since the values of the simulated circuit elements could not be measured by the available instruments, they were measured in different possible ways, such as a voltage divider circuit, parallel tuned circuit or an oscillator circuit.

The measured and calculated results were tabulated along with the discrepancies between them as percentage error. These results were plotted to give a better comparison between the experimental and theoretical observations. In addition, the working range of each circuit is reported.

The stability of some of these circuits was discussed using the non-idealities of the active elements. Two approaches were presented to study the instabilty of an inductor simulator circuit. Following one of these approaches, a circuit taken form literature [23] was proved to be unstable.

[1]The expression for the simulated circuit element is independent of V_T term

To conclude, one can say that the DiPTIT circuits presented in this thesis have attractive features. They are useful in a variety of ways and can find numerous applications. These circuits, specifically the inductor simulator circuits are very attractive from IC implementation point of view, since they can work at low frequencies and at the same time are much smaller in size (as IC) than a physical inductor working at those frequencies.

6.3 Directions for Future Work

Could something be done better? This is the question that most researchers ask themselves after they have investiagated and found solutions to their problems. The answer here is that as nothing is perfect and complete in this life, so are the DiPTIT circuits. Though they possess very attractive features, there is still a room for improvement and extension notably in three areas:

- The DiPTIT circuits should be designed to operate at high frequency such that they could be employed as front-end for radio recievers. In this case, current feedback operational amplifier (CFOA) and current conveyor (CC) would be useful active elements.

- A parallel tuned circuit could be designed, containing a voltage/current controlled simulated capacitor and inductor, such that the overall circuit becomes doubly tunable. This will give more control over the circuit parameters such

as frequency of oscillation or resonance frequency etc. However, stability problems would be a very sensitive issue in this case.

- The limited input voltage swing of the OTAs, restricts the range of values of the synthesised element obtainable from the simulator circuit. A technique could be devised to counter this problem, and hence increase the range.

Bibliography

[1] Umesh Kumar and Sushil Kumar Shukla. Analytical study of inductor simulation circuits. *Active and Passive Electronic Components*, 13:221–227, August 1989.

[2] A. Antoniou. Realization of gyrators using operational amplifiers and their use in RC-active network synthesis. *IEE Proceeding*, 116(11):1838–1850, 1969.

[3] Gary Sellani. Filter uses synthetic inductor. *Electronic Design*, pages 81–82, August 1993.

[4] Stephan I. Koutzarov. Digitally-controlled grounded inductance. *International Journal of Electronics*, 69(4):539–546, 1990.

[5] Ian Hickman. Negative approach to positive thinking. *Electronics World + Wireless World*, pages 258–261, March 1993.

[6] I.A. Khan et al. Novel wide-range electronically tunable ideal grounded inductance. *IEE Proceedings*, 135 Pt. G(3):104–106, June 1988.

[7] LTP Electronics. Current conveyor circuits. *Electronics World + Wireless World*, pages 962–963, November 1993.

[8] Dongming Qiu. Circuit design of an integralable simulated inductor and its applications. *IEEE Transactions on Instrumentation and Measurement*, 40(6):902–907, December 1991.

[9] Dongming Qiu. New simulated inductor using four-quadrant analogue multipliers. *International Journal of Electronics*, 75(6):1177–1184, 1993.

[10] Mckenny W. Egerton jr. No-loss tuned circuit. *Electronics World + Wireless World*, page 851, October 1993.

[11] K. Tabei et al. Realization of highly linear MOS circuits using negative impedance converters. *Electronics Letters*, 27(16):1416–1417, August 1991.

[12] S. Pipilos and Y. Tsividis. RLC active filters with electronically tunable centre frequency and quality factor. *Electronics Letters*, 30(6):472–474, March 1994.

[13] T. Vanisiri and C. Toumazou. The optoelectronic inductor: A new approach to high frequency, high Q active filters. *Electronics Letters*, 29(21):1878–1879, October 1993.

[14] Masaru Ishida et al. Grounded immitance simulation using single operational amplifier with a finite gain-bandwidth product. *Electronics and Communications in Japan*, 71 Part 1(1):39–46, 1988.

[15] R. Senani. On the synthesis of a class of immitances and filters using grounded capacitors. *International Journal of Circuit Theory and Application*, 11:410–415, 1983.

[16] A. Fabre et al. Current-controlled translinear impedance converter. *International Journal of Electronics*, 70(4):795–801, 1991.

[17] R.L. Brennan et al. The CMOS negative impedance converter. *IEEE Journal of solid-state circuits*, 23(5):1272–1275, October 1988.

[18] Sitthichai Pookaiyaudom and Kanok Samootrut. Efficient circuit implementation of current conveyors, negative impedance converters and nonlinear impedance converters using transconductance amplifiers. *International Journal of Electronics*, 64(6):941–945, 1988.

[19] Wanlop Surakampontorn et al. OTA-based electronically tunable voltage-controlled resistance converter. *International Journal of Electronics*, 67(1):81–85, 1989.

[20] S. Takagi et al. Improvement of differential amplifier CMRR using balanced-type NIC. *Electronics Letters*, 25(2):153–154, January 1989.

[21] Raj Senani and D.R. Bhaskar. Realization of voltage-controlled impedances. *IEEE Transactions on Circuits and Systems*, 38(9):1081–1086, September 1991.

[22] I.A. Khan and M.T. Ahmed. OTA-based integrable voltage/current-controlled ideal C- multiplier. *Electronics Letters*, 22(7):365–366, March 1986.

[23] A. Carlosena et al. Resistively variable capacitors using general impedance convertors. *IEE Proceedings-G*, 139(4):507–516, August 1992.

[24] John Dunn. Vary capacitance to positive or negative. *Electronic Design*, page 113, December 1991.

[25] Huang Qiuting et al. Design and implementation of a CMOS VCXO for FM stereo decoders. *IEEE Journal of Solid-State Circuits*, 23(3):784–793, June 1988.

[26] A. Carlosena et al. A new method for low-capacitance probing. *IEEE Transactions on Instrumentation and Measurement*, 42(3):775–778, June 1993.

[27] J. Silva-Martinez and E. Sanchez-Sinencio. Analogue OTA multiplier without input voltage swing restrictions and temperature-compensated. *Electronics Letters*, 22(11):599–600, May 1986.

[28] Randall L. Geiger and Edgar Sanchez-Sinencio. Active filter design using operational transconductance amplifiers: A tutorial. *IEEE Circuits and Devices Magazine*, 1:20–32, March 1985.

[29] Dan Ayers. The versatile world of OTAs. *Electronics World + Wireless World*, pages 197–201, March 1994.

[30] Angel Rodriguez et al. On the design of voltage-controlled sinusoidal oscillators using OTA's. *IEEE Transactions On Circuits And Systems*, 37(2):198–210, February 1990.

[31] Horacio Nevarez-Lozano et al. Frequency-limitations of continuous-time OTA-C filters. *Proceedings of IEEE International Symposium on Circuits and Sytems*, 3:2169–2172, June 1988.

[32] C. Acar. On the realization of OTA-C filters. *International Journal of Circuit Theory and Applications*, 21:331–341, 1993.

[33] B. Wilson. Recent developments in current conveyors and current-mode circuits. *IEE Proceedings*, 137, Pt. G(2):63–77, April 1990.

[34] A.S. Sedra et al. The current conveyor: History, progress and new results. *IEE Proceedings*, 137 Pt. G(2):78–87, April 1990.

[35] B. Wilson. Using current conveyors. *Electronics World + Wireless World*, pages 28–32, April 1986.

[36] Ahmed M. Soliman. Generalized immitance inverters and their realization. *International Journal of Electronics*, 41:59–64, 1976.

[37] Sedra & Smith. *Microelectronic Circuits.* Saunders College Publishers, 1990.

Vita

- Muhammad Haroon Khan
- Born in Multan, Pakistan
- Received Bachelor's degree in Electrical Engineering from the University of Engineering and Technology, Lahore, Pakistan in February, 1988.
- Worked as Assistant Manager (Design Engineer) in Telephone Industries of Pakistan (TIP), Haripur, Pakistan from June 1988 to March 1989.
- Worked as Assistant Engineer (Hardware Engineer) in Pakistan Space & Upper Atmosphere Research Commission (SUPARCO), Islamabad, Pakistan from March 1989 to May 1991.
- Completed Master's degree requirements at King Fahd University of Petroleum and Minerals, Dhahran, Saudi Arabia in October, 1994.